European Organization for Nuclear Research

SUMMER STUDENT REPORT

Physical and biological effectiveness studies on protons and heavy ions for use in FLASH radiotherapy

Student: Kristaps Paļskis

Supervisor: Mariusz Sapinski

August 2021

Contents

1 Introduction

Use of positively charged particle beams for radiotherapeutical treatment of cancer has been one of the main advancing fields of radiotherapy in 21st century. Over 100 treatment centers around the world are treating cancer patients with proton beams, utilizing the highly favorable dose deposition characteristics of protons – dose is mainly deposited in Bragg peak minimizing radiation exposure of normal tissue. Around 13 centers around the world are also using carbon ion beams that offer increased dose conformity compared to protons and attractive biological properies – increased relative biological effectiveness (RBE) compared to conventional photon treatments and lower oxygen enhancment ratio (OER) opening possibilities to treat hypoxic, radioresistant tumours, such as various sarcomas. Other ion species are also being investigated for clinical use, such as helium, oxygen, argon and others.

Another advancing field in radiotherapy that is of huge interest is the use of so called FLASH effect for treatment. In various studies it has been proved that using very high dose rate (FLASH) radiation (around 40-100 Gy/s) normal tissue damage from ionizing radiation is significantly lowered compared to conventional dose rate radiation treatment (around 3-6 Gy/min) while damage of tumor tissue remains at same level [1]. Therefore, FLASH effect offers lowered normal tissue complication propability (NTCP) while maintaining the same tumor control propability (TCP) or allows for possible tumor dose escalation. One of the main limiting factors of wide-spread FLASH therapy use is the various technological challenges it poses – delivery of very high dose per pulse and precise beam instrumentation at these highly elevated dose rate levels.

Although in proton therapy clinics most commonly used accelerator type is cyclotrons, in clinical heavy ion therapy currently only synchrotrons are used. For synchroton use in FLASH radiotherapy highly important parameter is the number of particles per spill – for stable FLASH dose rate delivery the whole treatment dose should be delivered in a single spill. Therefore it is of interest to understand the relation between necessary number of particles in a single spill and the various treatment parameters – tumor depth, tumor size, treatment dose level and used ion species.

The main aims of my summer student study therefore are:

- to identify impact of the mentioned treatment parameters on the necessary number of particles to achieve the desired dose distribution;

- to estimate the effectiveness of various ion species for treatment based on the dose distribution parameters like entrance dose and fragmentation tail dose distal to Bragg peak;
- to perform a literature review on ion biological effectiveness and estimate the biological effectiveness of various ion species and the biological parameter impact on the necessary number of particles for particular dose.

2 Materials and methods

2.1. Pristine Bragg peak Monte Carlo simulations

For all Monte Carlo (MC) simulation work in this study Geant4 simulation toolkit was used – particle transport simulation platform with applications in high energy, nuclear and accelerator physics and also medical physics and space science. Geant4 version 10.7. was used for simulations. For pristine Bragg peak simulations example code from Geant4 simulation package was used – hadronic physics example „Hadr01" [2].

Before MC simulations, neccessary particle entrance energies needed to be estimated based on the desired beam range in water. For this reason, relationship between beam entrance energy and mean energy loss range in water was established by calculations from numerically integrating Bethe-Bloch mean energy loss equation [3]:

$$-\frac{dE}{dx} = Kz^2 \frac{Z}{A}\frac{1}{\beta^2}\left[\frac{1}{2}\ln\frac{2m_e c^2\beta^2\gamma^2 T_{max}}{I^2} - \beta^2\right] \quad (2.1.)$$

$$K = 4\pi N_A {r_e}^2 m_e c^2 = 0.307\ MeV g^{-1} cm^2 \quad (2.2.)$$

$$T_{max} = \frac{2m_e c^2\beta^2\gamma^2}{1 + 2\gamma\frac{m_e}{M} + \left(\frac{m_e}{M}\right)^2} \quad (2.3.)$$

T_{max}: maximum transferable energy in a single collision;

z: Charge of incident particle;

M: mass of incident particle;

Z: charge number of medium;

A: Atomic mass of medium;

I: Mean excitation energy of medium;

N_A: Avogadro's number;

r_e: Classical electron radius;

m_e: electron mass (in keV);

β: relative velocity – v/c;

γ: Lorentz factor.

As Bethe-Bloch energy loss equation was used just for estimation of range in water in relation to entrance energy, no corrections were applied in equation (such as density,

shell corrections etc.). Medium for calculation was water and properties of this medium were chosen from NIST databases [4]:

- mean excitation energy I was set to 75 eV;
- Z/A ratio was set to 0.55508.

A simple, automated program for numerical integration of Bethe-Bloch equation was created in Visual Basic for MS Excel with and integration step dx set to 1 mm. Numerical integration procedure was performed for 6 different ion species chosen from SEEIST project report: protons (^{1}H), helium-3 (^{3}He), helium-4 (^{4}He), carbon (^{12}C), oxygen (^{16}O) and argon (^{32}Ar) ions. For each of the ion species initial particle kinetic energy per nucleon was chosen in steps of 1 MeV between minimum and maximum producable energy limits stated in NIMMS project note „*COMPARISON OF ACCELERATOR DESIGNS FOR AN ION THERAPY AND RESEARCH FACILITY*" (see Table 1.) [5]. After numerically integrated Bethe-Bloch equation curve was acquired the program was set to automatically calculate range in water for each of the energies – depth position with maximum energy loss. The acquired relationhips between intial particle kinetic energy per nucleon and range in water for various ion species is plotted in Figure 1.

Table 1. Main data from NIMMS project note [5] used for calculations in this study

		Particle type				
		^{1}H	^{4}He	^{12}C	^{16}O	^{36}Ar
Parameter	Lowest extraction energy [MeV/u]	60	60	100	100	200
	Highest extraction energy [MeV/u]	250	250	430	430	350
	Maximum number of particles per spill	$2.6*10^{11}$	$8.2*10^{10}$	$2*10^{10}$	$1.4*10^{10}$	$5*10^{9}$

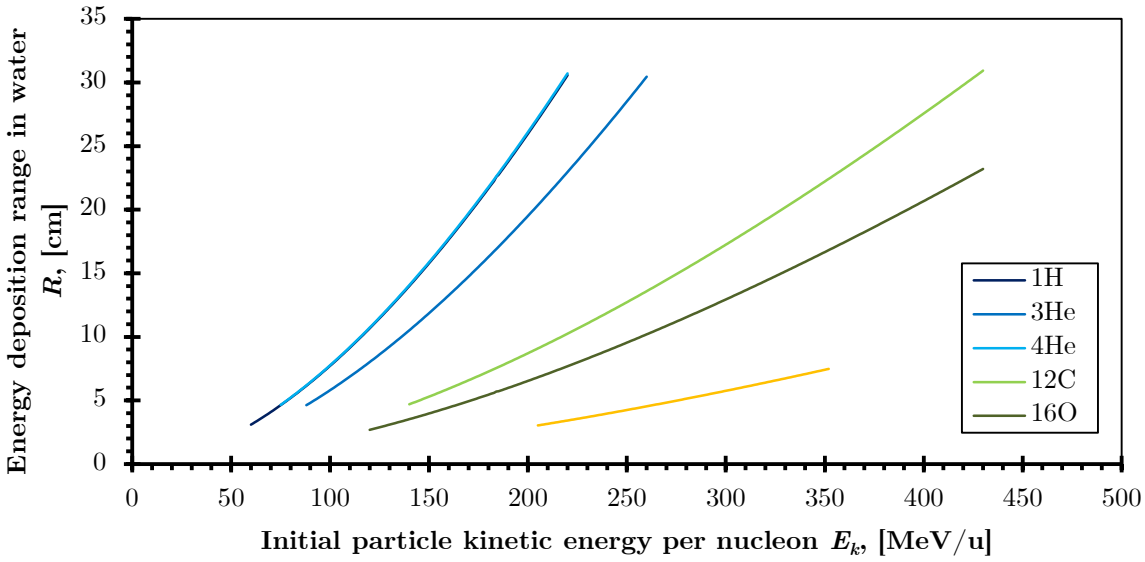

Figure 1. Calculated relationship between initial particle kinetic energy per nucleon and energy deposition range in water for various ion types

After acquiring this approximate relationship for various ion species, necessary input initial kinetic energies corresponding to range in water were calculated by linear interpolation between the calculated data points. Necessary kinetic initial kinetic energies were calculated for ranges between 50 to 250 mm in steps of 1 mm for all ion species except oxygen and argon ions, as their maximum initial kinetic energy was limited by technical specifications provided in NIMMS project note – necessary ranges of oxygen ions were between 50 to 220 mm and for argon ions – 28 to 71 mm. Maximum range of 250 mm was chosen for simulation of deeply seated tumors and range increment of 1 mm was chosen for appropriate spread-out Bragg peak (SOBP) optimization simulations in further steps of this study.

Having calculated all of the neccessary initial particle kinetic energies, MC simulations were performed. Simulations were performed without assuming any specific accelerator beamline, simply simulating pencil-like beams. The geometry of the simulation was:

- scoring volume (Target) was set to be a cylinder with a length of 300 mm and a radius of 200 mm. Volume is divided in „discs" of 1 mm length for energy deposition scoring. The material of scoring volume was water (G4_WATER).
- scoring volume was placed in an environmental volume (World) that extends 10 mm from scoring volume in all directions. The material of environmental volume was air (G4_AIR).

Particle emmision was simulated from a point-like source placed 5 mm above scoring volume entrance surface on central axis of scoring volume and initial particles were assumed to have the same initial kinetic energy without any energy spread.

For choosing appropriate physics process list for running MC simulations a literature review was performed. Studies [6][7] have shown that for particle energy range that is of interest in proton and heavy ion therapy it is recommended to use either QGSP_BERT, QGSP_BIC or FTFP_BERT physics lists for MC simulations. Initial simulations were made for comparison between results of these 3 physics lists and it agreed with results from literature – differences between these different simulations are less than 1% [7]. Since such a difference is neglible, QGSP_BIC physics list was chosen for all of the pristine Bragg peak simulations simply because of faster performance. QGSP_BIC physics list uses Geant4 Binary cascade for primary protons and neutrons with energies below ~10GeV, thus replacing the use of the low energy parametrised (LEP) model for protons and neutrons - binary cascade better describes production of secondary particles produced in interactions of protons and neutrons with nuclei. It also uses the binary light ion cascade to model inelastic interaction of ions up to few GeV/nucleon with matter.

For all of the individual MC simulation runs of each initial particle kinetic energy 10^5 histories were simulated and secondary particle production was not supressed, cuts of electromagnetic process were left to default values. After each of simulation runs a ROOT file containing histograms was created – using ROOT framework energy deposition (MeV/mm) histogram was exported from each of the simulation runs to a TXT file for further actions and calculations. ROOT version 6.24/00 was used.

2.2. Spread-out Bragg peak design – physical dose optimization

For design of spread-out Bragg peaks (SOBP) an optimization of weights for each of the individual pristine Bragg peaks was performed. For each of the ion species studied, except argon ions, two sets of SOBP's were created simulating deeply seated tumors (maximum distal range of 25 cm, for oxygen ions – 22 cm) and medium depth tumors (maximum distal range of 15 cm), to study the impact of SOBP maximum depth on various physical parameters of the dose distribution. In each of the sets SOBP length was varied from 1 to 10 cm in steps of 1 cm, to study the impact of SOBP size on dose distribution. To study the difference between all of the ion types, a shallow SOBP was calculated as well, with distal edge at 7 cm depth and proximal edge at 5 cm depth, therefore allowing argon ions to be included in the comparison.

Optimization of pristine Bragg peak weights was performed using least squares method:

- each of the pristine Bragg peaks that have a Bragg peak position in the range of a particular SOBP were assigned a starting weight with value of 1, all the other peaks in a set – a weight of 0;
- energy deposition at a particular depth was multiplied by the weight of the particular pristine Bragg peak and summed over all of pristine peaks in the set for each depth – total energy deposition;
- total energy deposition curve was normalized to the maximum value in curve;
- a step function was defined simulating „ideal" SOBP curve – having a value of „1" at all depths corresponding to a particular SOBP;
- objective function was defined for optimization using least squares method:

$$\sum_{i=p}^{d}(E_{i\,tot.norm} - 1)^2 \rightarrow min \qquad (2.4.)$$

p – depth of proximal edge of SOBP;

d – depth of distal edge of SOBP;

$E_{i\ tot.norm}$ – normalized total energy deposition at depth i.

- as an optimization constraint it was defined that sum of all individual pristine Bragg peak weights must equal a value of 1 as that allows straight-forward derivation of number of particles from SOBP energy deposition distribution.

Optimization procedure of the objective function that was set-up previously was performed in MS Excel environment using Solver tool. Each of the pristine Bragg peak sets for optimization contained energies with ranges in steps of 1 mm.

For any energy deposition conversion into absorbed dose a simple calculation was performed:

$$D = \frac{E_{deposited}}{m} = \frac{E[MeV] * 1.6022 * 10^{-13}}{V * \rho}, \text{where} \qquad (2.5.)$$

E[MeV] – deposited energy at certain depth in MeV units;

V – volume of the element of interest, in this study used cuboid of thickness 1 mm (according to simulation data) and crossection changed accordingly (usually 10 x 10 cm, simulating 10x10x10 cm tumor volume);

ρ – material density, in this study water – density of 1000 kg/m^3.

2.3. Theoretical introduction on relative biological effectiveness. Calculation of relative biological effectiveness.

As protons and heavy ions are particles having an increased linear energy transfer (LET), these particles exhibit increased relative biological effectiveness in living tissue – smaller physical absorbed dose is necessary for protons and heavy ions to provide the same cell survival level as a reference radiation, for reference radiation ususally a 200 kVp or ^{60}Co beam is used. Therefore:

$$RBE = \frac{D_{ref}(S)}{D(S)} \tag{2.6.}$$

$D_{ref}(S)$ – absorbed dose of reference radiation providing a survival level of a value S;

D(S) – absorbed dose of a particular ion species providing a survival level of a value S.

Relative biological effectiveness is a complicated function depending on various parameters: radiation properties, total delivered dose and dose fractionation scheme, dose rate, studied cell parameters and biological endpoint for RBE calculation [8]. It must be noted that RBE is typically higher at lower dose per fraction and for cell mutations rather than cell killing.

Various studies have shown that for protons and heavy ions RBE increases with increasing linear energy transfer. LET is a macroscopic property of dose deposition characterizing locally deposited energy dE by transversing a distance dl. In definition LET is similiar to „stopping power", though the main diference is that in „stopping power" calculation energy deposition is divided over absorber thickness, rather that in the case of LET – over particle track length. As per ICRU reports, in LET calculation only electronic stopping energy losses are to be considered [8]. LET values greatly increase at the end of particle track – around Bragg peak. In medical physics dosimetry two types of LET calculations are distinguished:

- track-averaged LET_t – arithmetic mean value of LET fluence spectrum (dose deposited over fluence);
- dose-averaged LET_d – using dose of each individual energy deposition as weighting factor of LET spectrum.

As already mentioned, it has been shown that RBE values tend to increase with increasing LET values – slow increase when LET is lower than 10 keV/μm, faster increase in the range till about 100 – 200 keV/μm and after that a plateau is reached

in RBE value that is followed by a decrease of RBE with increasing LET value. The plateau and decrease of RBE value for very high LET radiation is explained by the so called „overkill" effect – with higher LET than optimal value for DNA strand breaks, dose is deposited even more locally around initial particle track and more local ionizations events have happened that do not cause DNA damage – so called „wasted dose" [9].

Although, it was mentioned that there is a trend in relationship between RBE and LET, no clear and certain calculation models have been made created connecting the two parameters. Main reasons for that are coming from the fact that RBE is highly dependant on biological endpoint and it differs by atomic number of the particle – different particles with same LET value do not neccesarily have the same RBE value. Several phenomenological models have been created relating the 2 parameters, though it must be noted that usually these models are valid only for one certain type of particle and limitations of such models must be carefully evaluated before using them for biological dose estimation.

In clinical medical physics RBE calculations typically are done using one of two models for more precise estimation of the biological effect of the treatment: Local Effect Model (LEM) and Microdosimetric Kinetic Model (MKM).

- Local Effect Model [10] – main aim of model is derivation of ion radiation biological effects from response of cells to conventional photon radiation. Main concept in this model is „local dose" (sometimes reffered as „radial dose profile") – expectation of energy deposition at any position in radiation field for a known particle trajectories. The local dose distribution is derived from using particle track structure as representation for energy deposition – a function of energy deposition dependent on radial distance to the particle trajectory. The model assumes that equal local doses lead to equal local biological effects without the need to include radiation quality in calculation and effectiveness is calculated on basis of this microscopic local dose deposition pattern of ions traversing the cell nucleus by integration of local dose deposition density. Local dose distributions of radial dose profiles can be derived using Monte Carlo simulations, although analytical solutions have been proposed for faster estimation of local dose deposition characteristics. LEM is used as biological dose estimation algorithm at GSI facility.
- Microdosimetric Kinetic model [11] – biological basis of the model is dividing cell nucleus into smaller subcellular regions reffered as „domains" and assuming two types of possible ionizing radiation damage – type I lesion, which is always lethal for the cell, and type II lesion, which is potentially

lethal but can be correctaly repaired (DNA double strand breaks). Number of lesions for both types is proportional to a microdosimetric parameter – specific energy z. Specific energy is stochastic, microdosimetric parameter that is defined as energy deposited by ionizing radiation to a small volume of mass. MKM has been also revised and extendended to include saturation corrections of specific energy to account for decrease of RBE caused by the overkill effect. It must be noted that saturation corrections of specific energy are dependent on cellular stucture parameters used in model – radius of the whole cell nucleus and corresponding domain radius. This and other biological parameters are derived by fitting MKM results to data acquired in cell irradiation experiments, indicating that distinct data set is required for each of different cell types. MKM is used as biological dose estimation algorithm at HIMAC facility and MKM was also used as biological dose calculation model in this study. Further mathematical description of MKM is provided, regarding the use of it in this study.

According to MKM, number of lethal lesions L_n in the cell nucleus can be calculated as [12]:

$$L_n = (\alpha_0 + \beta z_{1D}^*)D * \beta D^2, \text{where} \tag{2.7.}$$

$\alpha 0$ – constant, representing initial slope of survival curve in the limit, when LET=0;

β – constant, independent of the radiation type;

D – absorbed dose;

z^*_{1D} – saturation-corrected dose-mean specific energy of the domain delivered in a single event [12]:

$$z_{1D}^* = \frac{\int_0^\infty z_{sat} f_1(z) dz}{\int_0^\infty z f_1(z) dz}, \text{where} \tag{2.8}$$

$f_1(z)$ – propability density of z deposited by a single energy-depostion event of the domain;

z_{sat} – saturation-corrected specific energy:

$$z_{sat} = \frac{{z_0}^2}{z}\left(1 - e^{-\frac{z^2}{{z_0}^2}}\right), \text{where} \tag{2.9.}$$

z_0 – saturation coeffficient:

$$z_0 = \frac{\left({R_n}/{r_d}\right)^2}{\sqrt{\beta\left(1+\left({R_n}/{r_d}\right)^2\right)}}, \text{where} \tag{2.10.}$$

R_n – radius of cell nucleus of interest in calculation;

r_d – radius of the subcellular domain in nucleus.

Regarding specific cell biological parameters, as was already mentioned, are different for each type of cell type. One of the main cell line types appearing in various radiobiology studies is human salivary gland (HSG) cell line – this cell line was also chosen for simulation studies in this work. MKM parameters that are predefined for HSG cell line, according to calculation done in other studies [12]:

- α_0 – 0.172 Gy^{-1};
- β – 0.05 Gy^{-2};
- R_N – 3.9 μm;
- r_d – 0.32 μm.

Data on saturation-corrected dose-mean specific energies irradiating HSG cell line were taken from [12]. The data includes saturation-corrected dose-mean specific energy values for various ions with different atomic number and in dependence of particle energy per nucleon. Visual representation of this data is given in Figure 2.

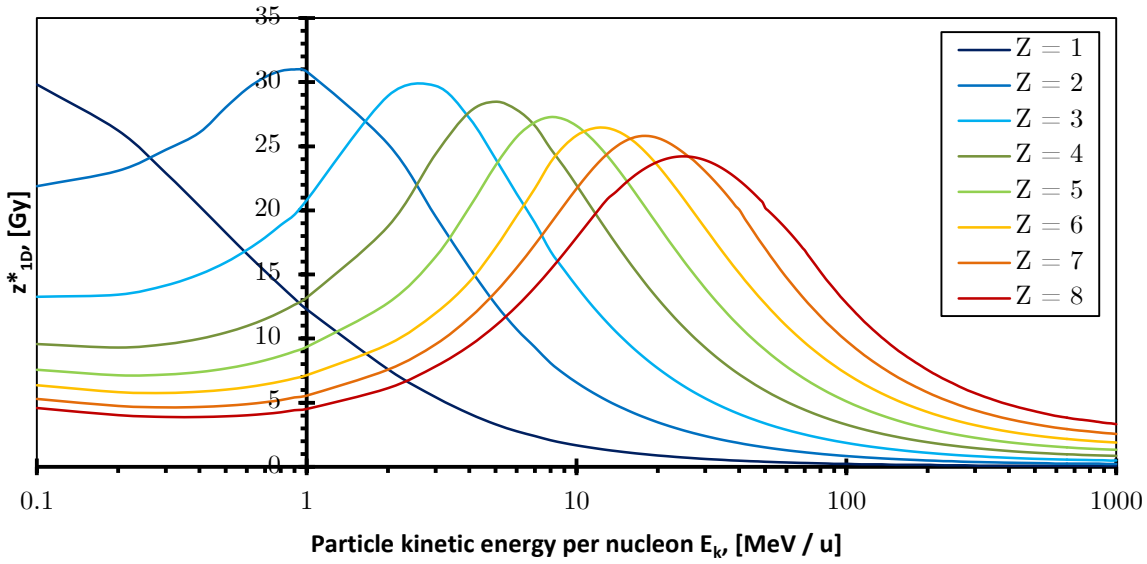

Figure 2. Saturation-corrected dose-mean specific energy as function of particle kinetic energy per nucleon for ions wih atomic number in range 1 to 8

In regards to actual RBE calculation, RBE from MKM is given by [12]:

$$RBE = D_{ref}(S) \Big/ \left[\frac{-(\alpha_0 + \beta z_{1D}^*) + \sqrt{(\alpha_0 + \beta z_{1D}^*)^2 - 4\ln(S)\beta}}{2\beta} \right], \text{where} \quad (2.11.)$$

$D_{ref}(S)$ – absorbed dose of reference ionizing radiation at survial fraction;

S – survival level from curve for reference ionizing radiation quality

In regards to RBE value calculation, one of the main aspects that needs to be calculated from physical properties of particle beam is the distribution of saturation-corrected dose-mean specific energy. For calculation of that it is necessary to have information on kinetic energies of particles. It must also be pointed out, that for heavier ions beam fragmentation is present and is of great importance - because of ion beam fragmentation, particles with an atomic number different from primary particle are present in radiation field and kinetic energy distributions of such secondary particles are also very different from primary particles. Therefore for a precise RBE calculation saturation-corrected dose-mean specific energy should be calculated for each particle of different atomic number indepenedently and only afterwards a sum should be made. In spite of that, in this study only RBE of primary particles was calculated, since the contribution from primary particles defines main part of RBE value. Impact of not including secondary fragment particles in RBE calculation was further discussed at the end of study in Results section.

For calculation of kinetic energy of primary beam particles MC simulations were run in Geant4 platform. Custom-code was created for this calculation based on Hadr01 example code for scoring kinetic energy at each of scoring volume subvolumes (discs). Secondary particle transport was turned off for these simulations (using command KillAllSecondaries) ensuring that only primary particles were scored. MC simulations of kinetic energy depth distribution were run for all of the initial energies calculated in 2.1. step for each of the particle types.

After the kinetic energy distribution was calculated for each of particles studied, saturation-corrected dose-mean specific energy distribution of each pristine Bragg peak was calculated. For kinetic energy in each depth corresponding value of specific energy was found by linear interpolation of the full data table of saturation-corrected dose-mean specific energy in relation to particle kinetic energy for the specific particle, considering its atomic number.

The next steps for RBE calculations based on energy deposition curves:

- energy deposition curves are normalized to maximum value and used as dose deposition curves. Dose deposition curves are then calculated, depositing certain dose level spread-out region.

- these physical dose deposition curves are then used for calculation of survival curves for irradiation with reference radiation of 200 kVp photons. Inserting α and β values corresponding to HSG cell lines, cell survival S curve can be calculated from dose D curve by formula:

$$S = e^{-(0.172D*0.05D^2)} \quad (2.12.)$$

- using the calculated cell survival curve and the corresponding dose curve, RBE value curve is calculated by formula 2.11.;
- biologically effective dose is calculated by multiplying the physical dose deposition curve with RBE value curve.

2.4. Spread-out Bragg peak design – biologically effective dose optimization

Because of the variable RBE values in SOBPs of heavy charged particles, in order to maintain uniform biologically effective dose in SOBP region the physical dose distribution delivered must be optimized to provide a dose profile compensating for RBE variation. Main steps of this process are already discussed in paragraphs 2.2. and 2.3., to reiterate:

- each of the pristine Bragg peaks with position in the range of a particular SOBP were assigned a starting weight with value of 1, others – 0;
- energy deposition at a particular depth was multiplied by the weight of the particular pristine Bragg peak and summed for each depth – total energy deposition – physical dose;
- an optimization constraint was defined - sum of all individual pristine Bragg peak weights must equal a value of 1;
- total energy deposition curve is normalized to the maximum value in curve and multiplied by a number (variable during optimization process) – simulating physical dose;
- saturation-corrected dose-mean specific energy values that are defined at each depth for pristine Bragg peaks are also multiplied by the same weight of the the particular peak and summed at each depth – specific energy value for whole SOBP;
- based on physical dose curve – survival curve is calculated – and afterwards RBE value at each depth, which is multiplied by physical dose to give biologically effective dose D_{bio};

- a step function was defined simulating „ideal" biologically effective SOBP curve – having a value of the prescribed dose $D_{prescribed}$ at all depths corresponding to a particular SOBP;
- objective function was defined for optimization using least squares method:

$$\sum_{i=p}^{d}\left(D_{i\,Bio} - D_{prescribed}\right)^2 \rightarrow min \qquad (2.13.)$$

Biologically effective dose optimized SOBPs were created for all particle types in this study for:

- deep-seated SOBPs with distal edge at 250 mm and shallower SOBPs with distal edge at 150 mm;
- for both depth groups – SOBPs of 5 and 10 cm length were considered;
- for each depth and SOBP size combination biologically effective dose SOBPs were optimized for prescribed dose levels of 2, 5, 10 and 20 Gy.

3 Results

3.1. Simulated pristine Bragg peak sets for various ions

In figures 3. to 8. sets of simulated pristine Bragg peaks for various ions are given, having particle ranges that were set in Paragraph 2.1. For each ion type to figures are given – full set of pristine Bragg peaks and reduced set having pristine Bragg peaks with range in steps of 10 mm (for better visual representation to see changes in peak shape). Pristine Bragg peaks are not normalized, representing actual energy deposition values.

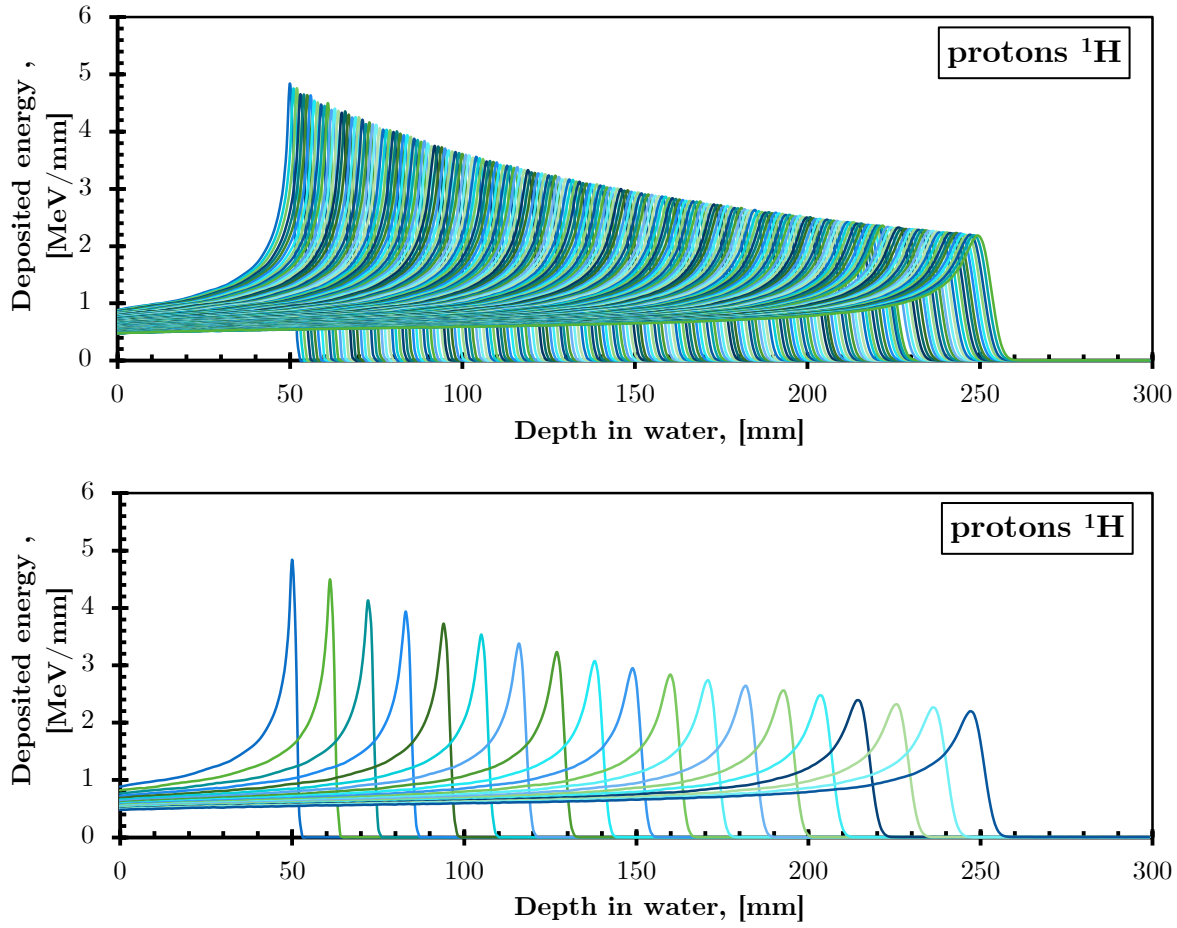

Figure 3. Simulated pristine Bragg peak set for protons ^{1}H:

upper full set, *lower* pristine Bragg peaks with range increasing in steps of 10 mm

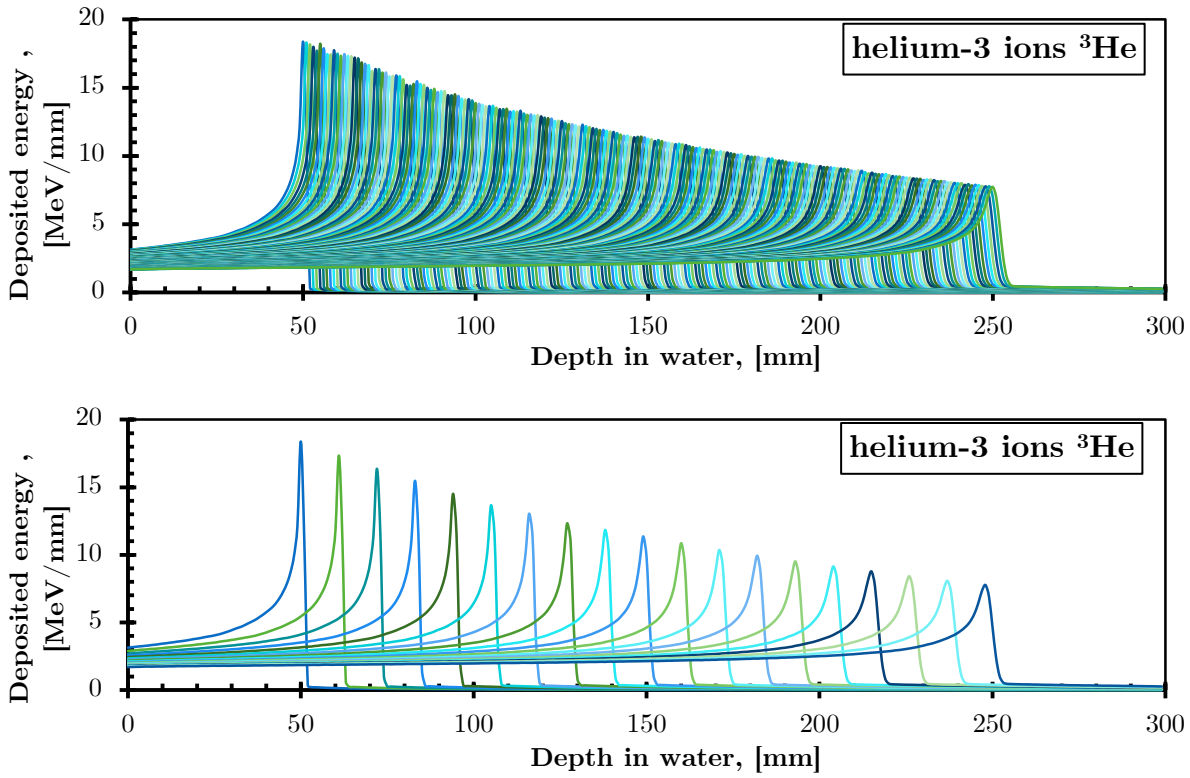

Figure 4. Simulated pristine Bragg peak set for helium-3 ions ^{3}He:

upper full set, *lower* pristine Bragg peaks with range increasing in steps of 10 mm

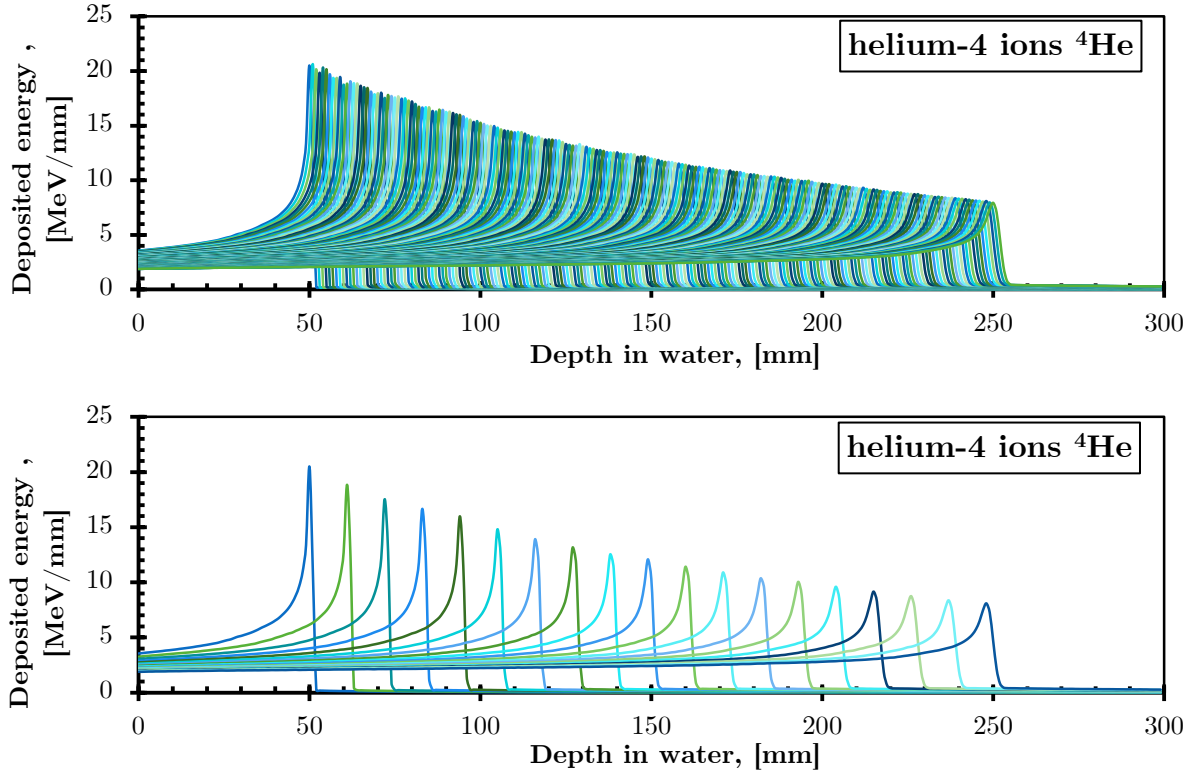

Figure 5. Simulated pristine Bragg peak set for helium-4 ions ^{4}He:

upper full set, *lower* pristine Bragg peaks with range increasing in steps of 10 mm

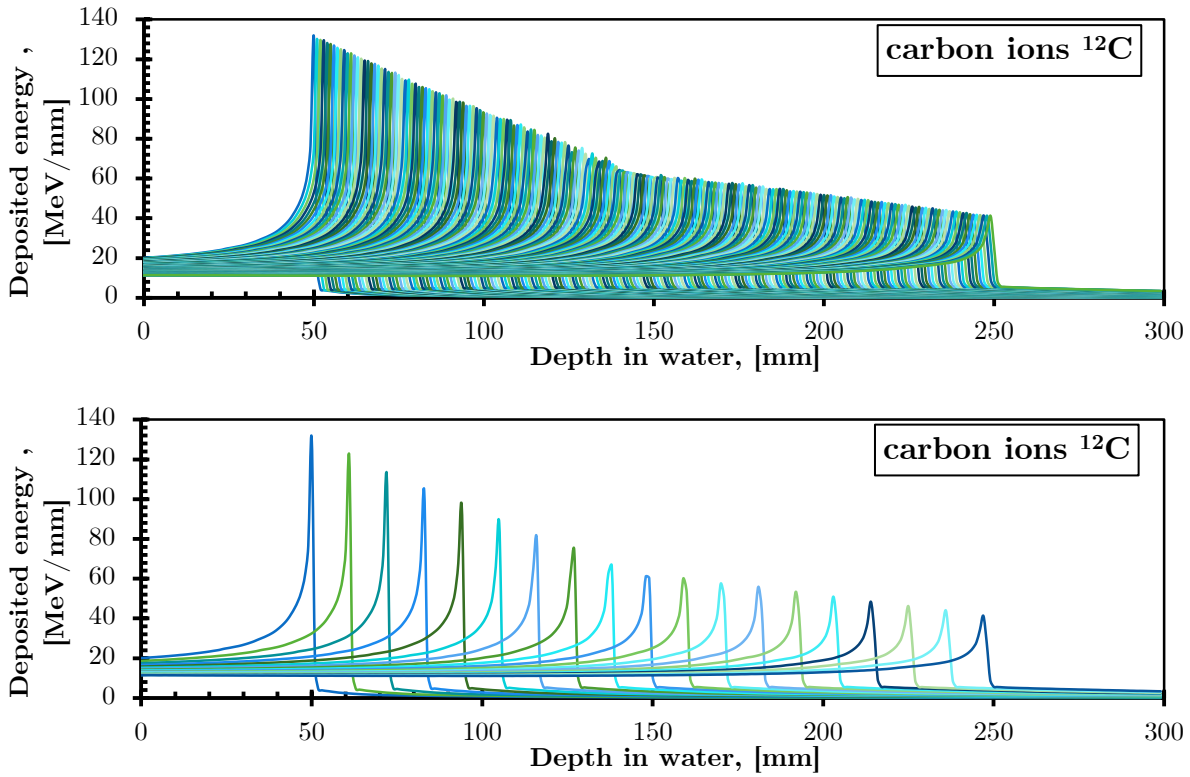

Figure 6. Simulated pristine Bragg peak set for carbon ions ^{12}C:

upper full set, *lower* pristine Bragg peaks with range increasing in steps of 10 mm

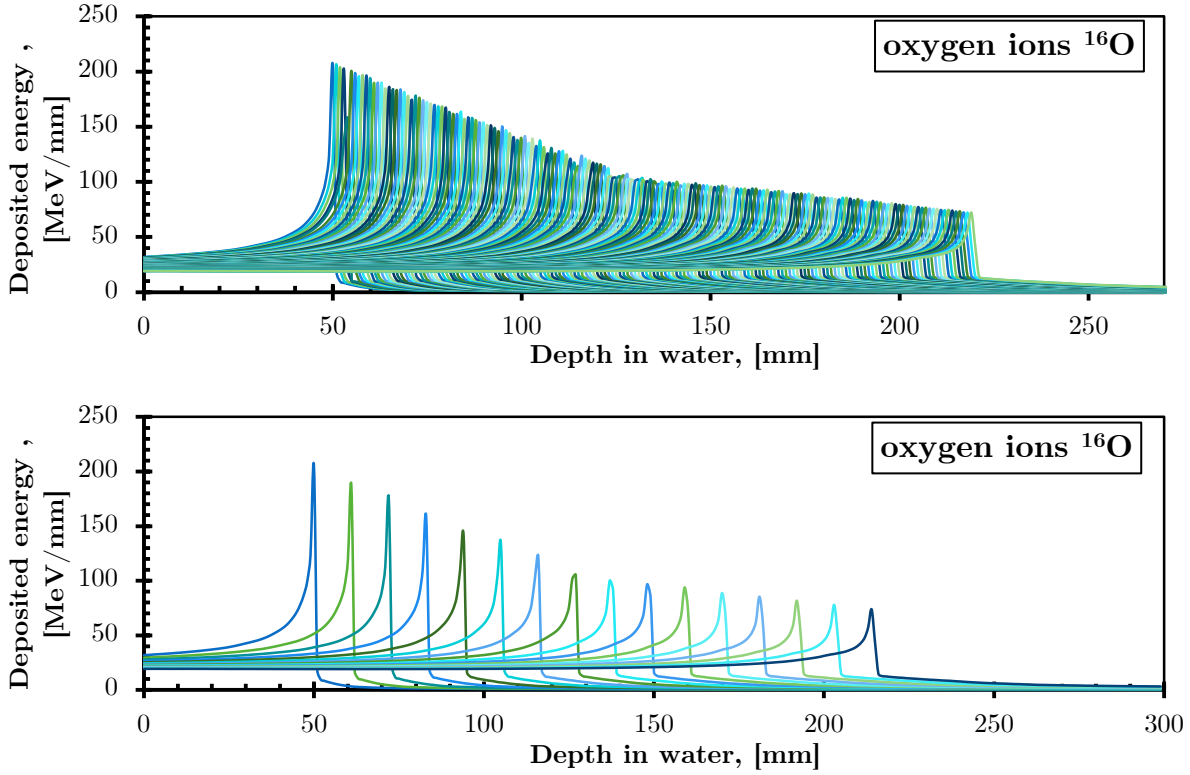

Figure 7. Simulated pristine Bragg peak set for oxygen ions ^{16}O:

upper full set, *lower* pristine Bragg peaks with range increasing in steps of 10 mm

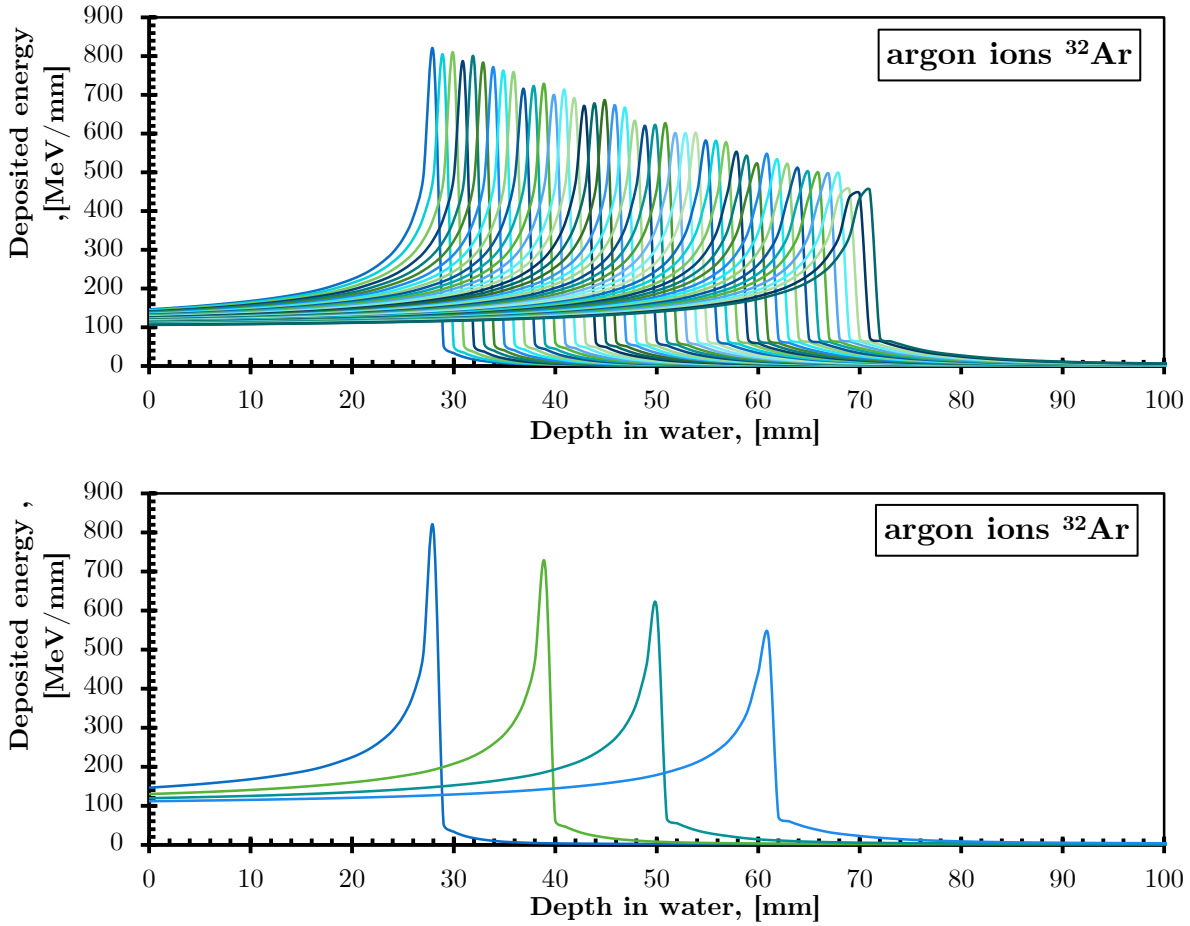

Figure 8. Simulated pristine Bragg peak set for argon ions ^{32}Ar:

upper full set, *lower* pristine Bragg peaks with range increasing in steps of 10 mm

Using data for energy deposition of the simulated Bragg peaks and number of particles per spill according to Table 1, absorbed dose curves were calculated for pristine Bragg peaks of 250 mm range – simulating deep-seated tumors (for oxygen ions – 220 mm, limitation of maximum energy). Calculated absorbed dose curves are given in Figure 9.

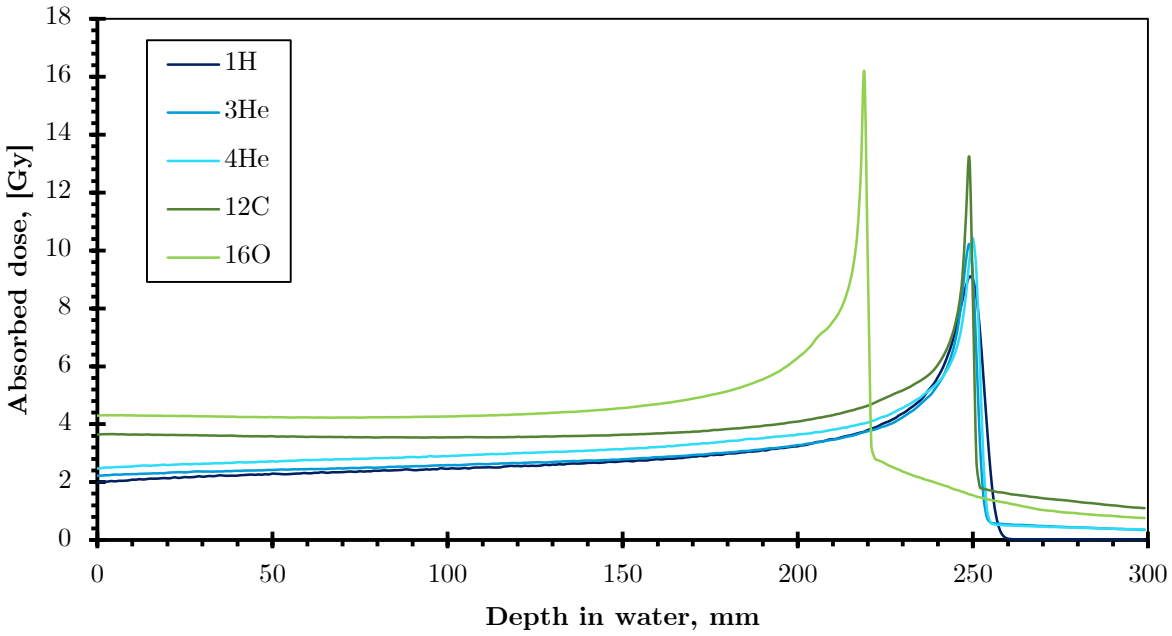

Figure 9. Absorbed dose curves for particles with range of 250 mm (220 for oxygen), using data from NIMMS report

All of the simulated pristine Bragg peak data sets show two of the main things regarding heavy charged particle physics for treatment:

- with increasing range (increasing initial particle energy) the maximum energy deposition value decreases and Bragg peak regions becomes wider – so called range and energy straggling resulting from stochastic nature of energy loss process. Widening of Bragg peak also points to increase of beam lateral spread. From this there is clear indication of rationale of heavier charged particles – with increasing particle mass both the energy and range straggling and lateral beam spread decreases, therefore allowing more conformal dose deposition. Though – this aspect of heavier particle effectiveness is not further discussed or studied in this work.
- for particles heavier than protons secondary particle generation and so called fragmentation increases – for heavier particles there is increased energy deposition beyond Bragg peak because of these secondary fragments. Secondary particle contribution in „tail region" increases with increasing initial particle energy and become more pronounced with increasing atomic number of the primary particle.

3.2. Spread-out Bragg peaks based on physical dose optimization

In figure 10. example of results of SOBP mathmetical optimization are given for protons and carbon ions – total SOBP and weighted individual peaks. In figures 11. to 15. visual representations of mathematically optimized SOBPs are given for various ion types, based solely on optimizing just the physical dose distributions and not taking any biological effectiveness values into account. SOBPs optimization results are given with SOBP length in range of 1 to 10 cm in steps of 1 cm. Two sets are provided for each ion type, according to 2.2. paragraph – with SOBP distal edge fixed at 15 and 25 cm depth (for oxygen ions 15 and 22 cm depth).

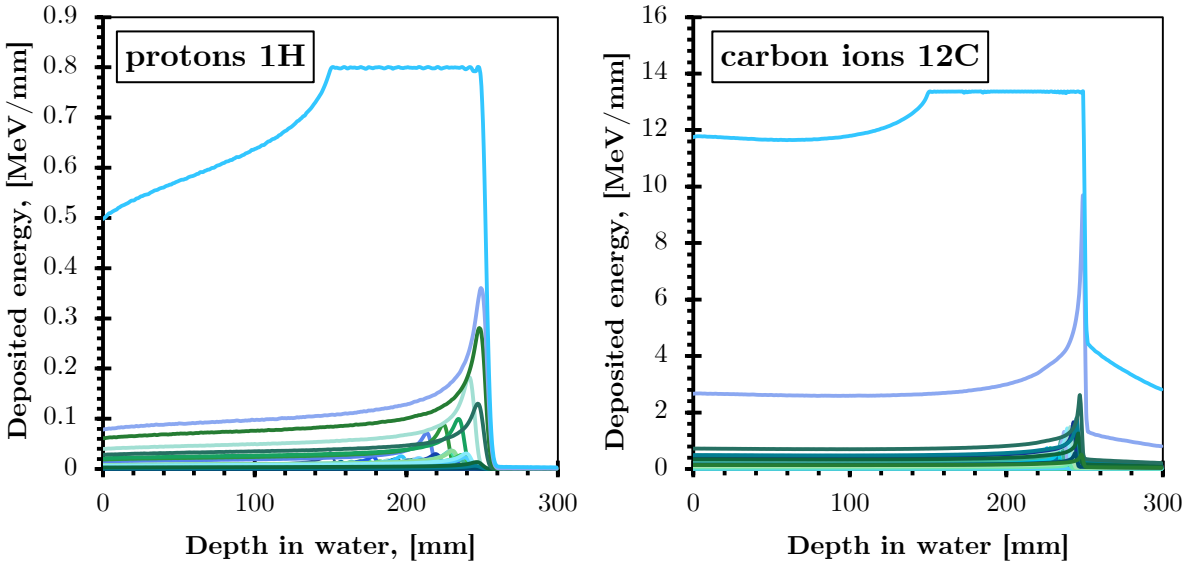

Figure 10. Physical dose optimized spread-out Bragg peaks and weighted individual pristine Bragg peaks for 10 cm SOBP with distal edge at 25 cm depth:

left for protons, *upper* for carbon ions

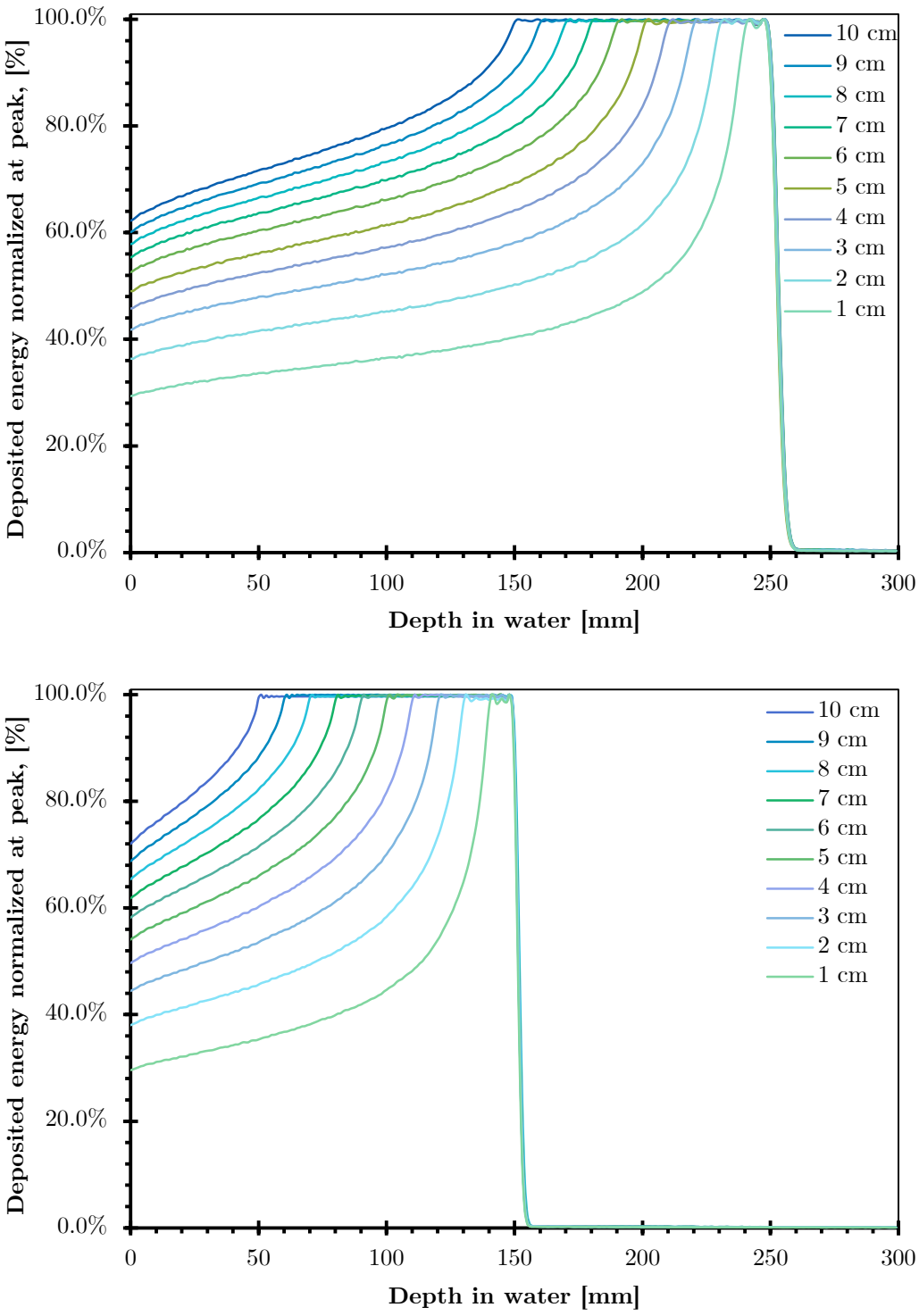

Figure 11. Physical dose optimized spread-out Bragg peaks for protons ^{1}H with different peak lengths:

upper peak distal edge fixed at 25 cm depth, *lower* peak distal edge fixed at 15 cm depth

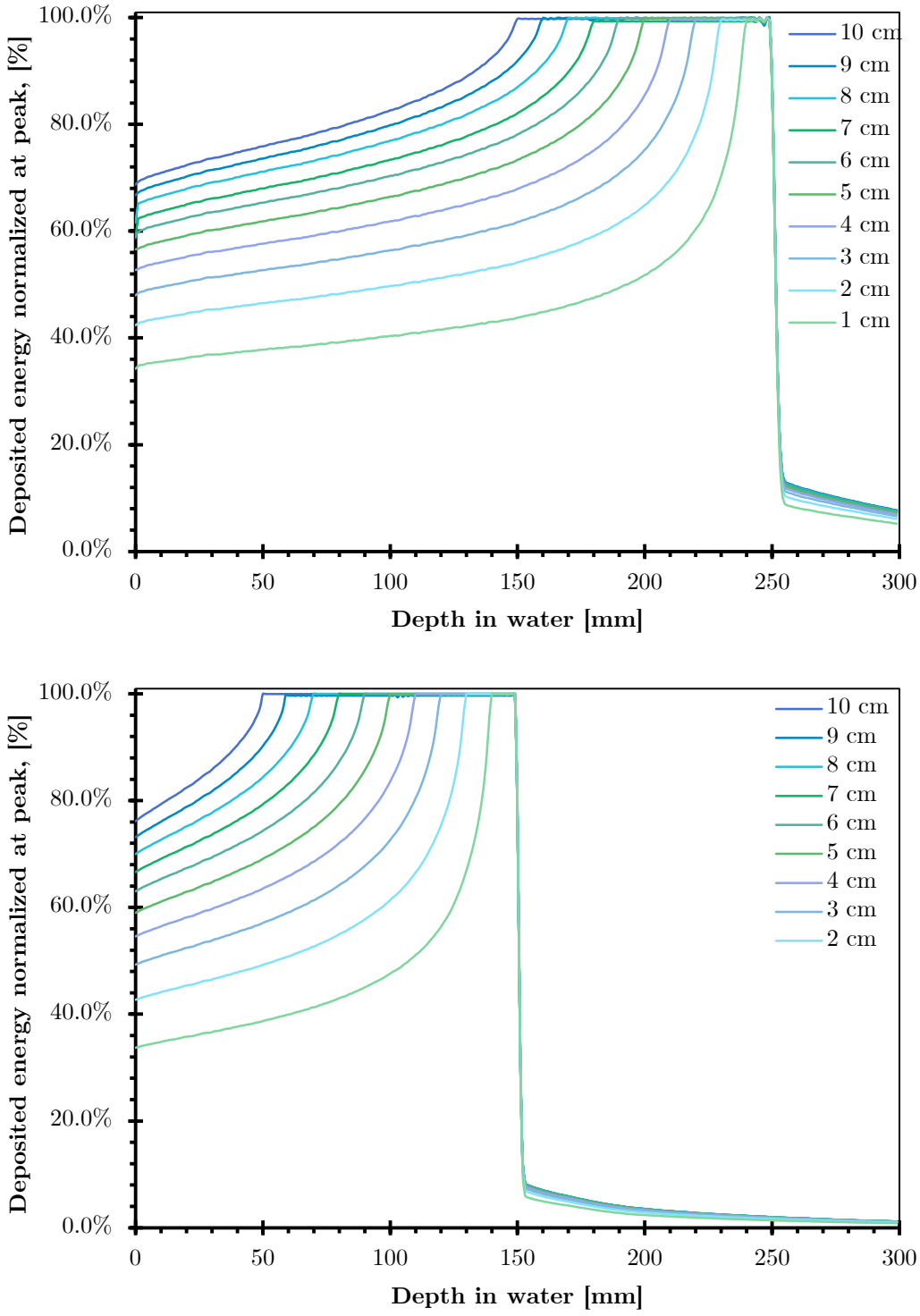

Figure 12. Physical dose optimized spread-out Bragg peaks for helium-3 ions ^{3}He with different peak lengths:

upper peak distal edge fixed at 25 cm depth, *lower* peak distal edge fixed at 15 cm depth

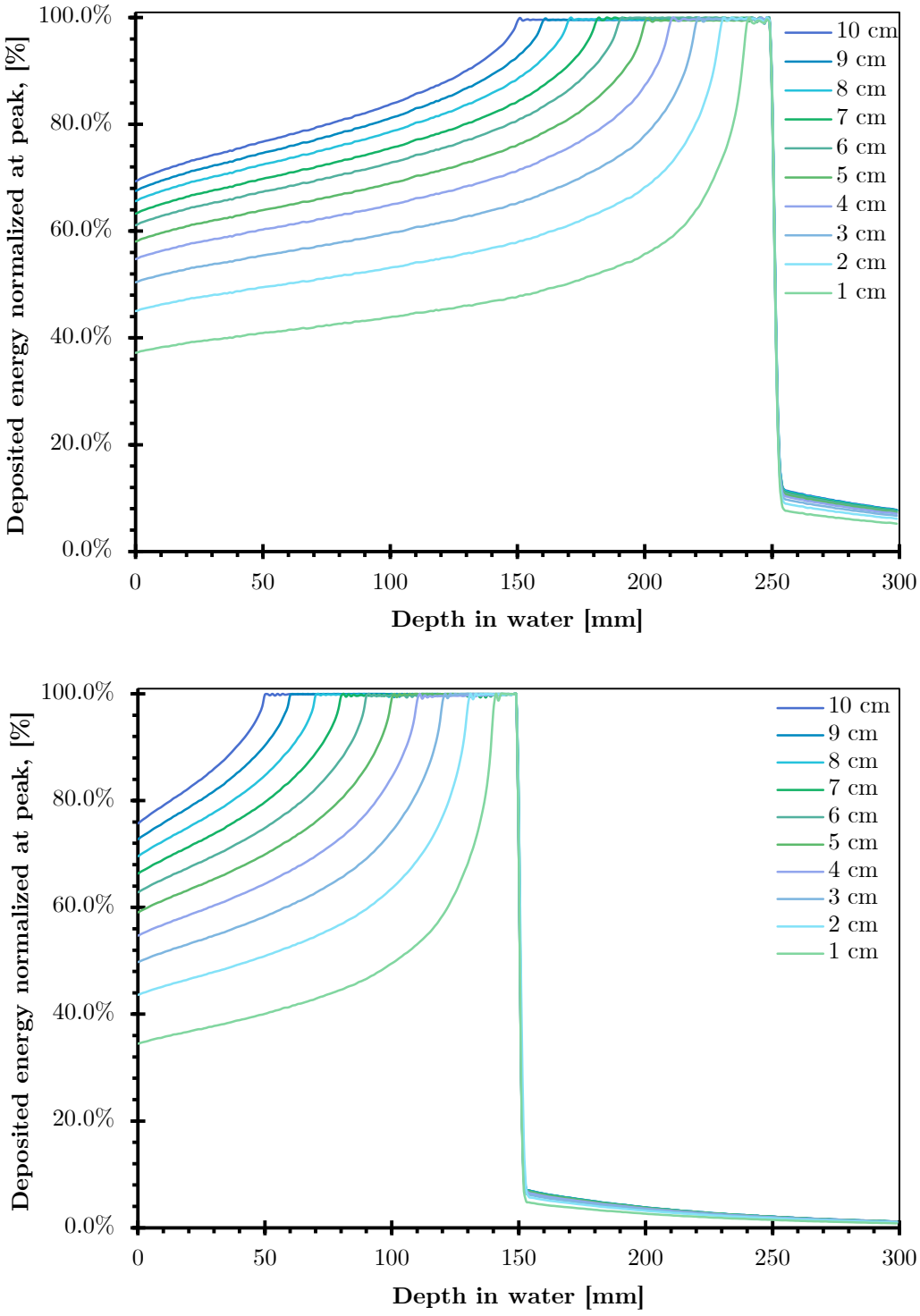

Figure 13. Physical dose optimized spread-out Bragg peaks for helium-4 ions ^{4}He with different peak lengths:

upper peak distal edge fixed at 25 cm depth, *lower* peak distal edge fixed at 15 cm depth

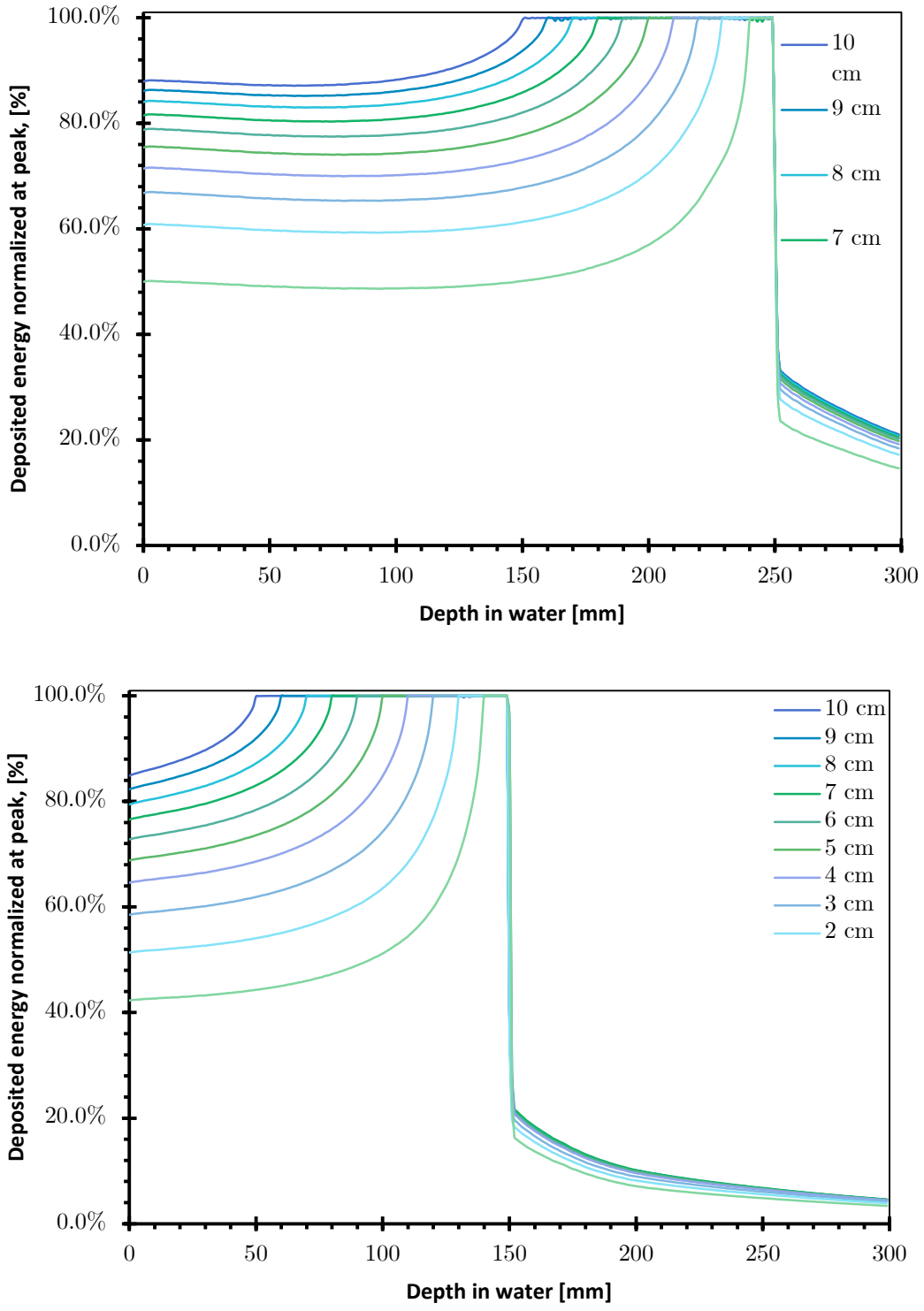

Figure 14. Physical dose optimized spread-out Bragg peaks for carbon ions ^{12}C with different peak lengths:

upper peak distal edge fixed at 25 cm depth, *lower* peak distal edge fixed at 15 cm depth

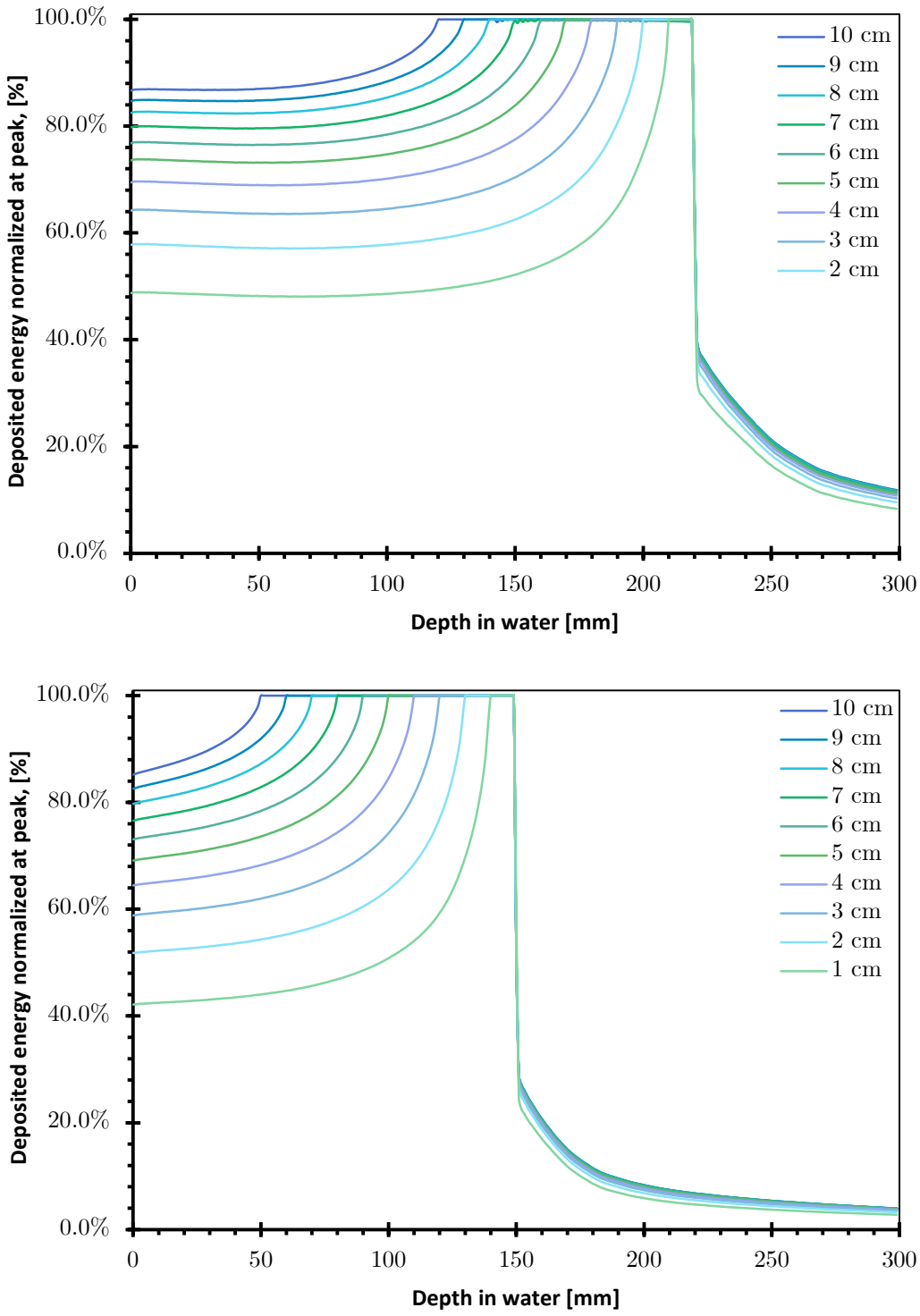

Figure 15. Physical dose optimized spread-out Bragg peaks for oxygen ions ^{16}O with different peak lengths:

upper peak distal edge fixed at 25 cm depth, *lower* peak distal edge fixed at 15 cm depth

In figures 16. to 18. physical dose optimized SOBPs from previous step for different ion types are compared between each other. Various depths of distal edge were chosen because of the limitations on beam energies discussed in this study as discussed in 2.1. paragraph.

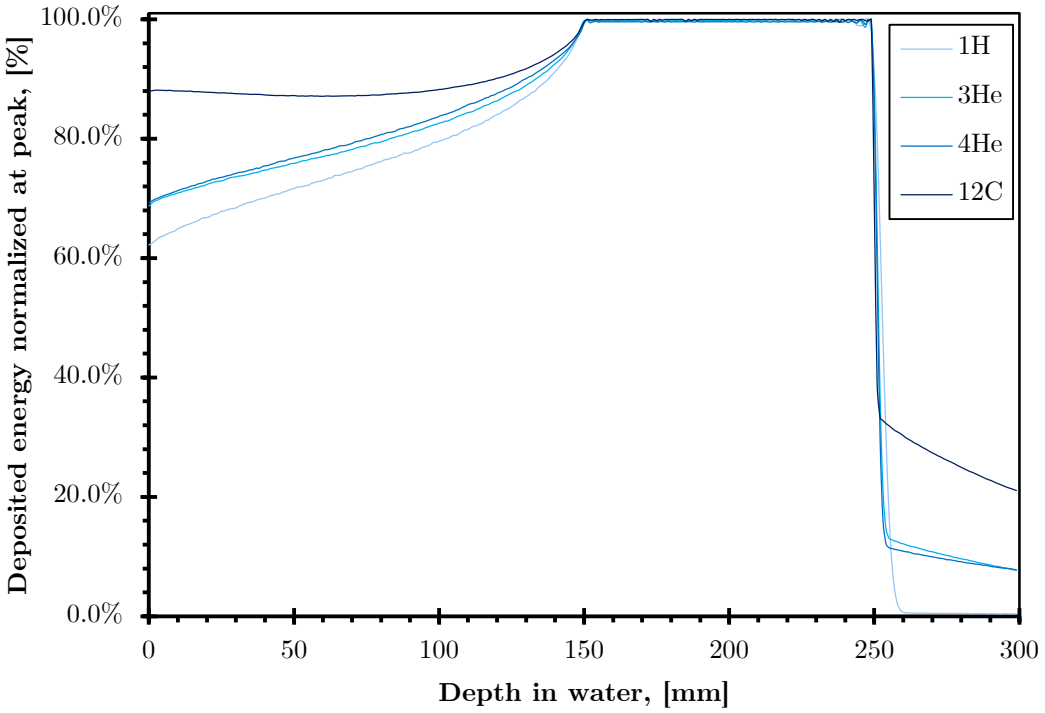

Figure 16. Physical dose optimized spread-out Bragg peak comparison for different ions: SOBP of 10 cm length with distal edge at 25 cm depth

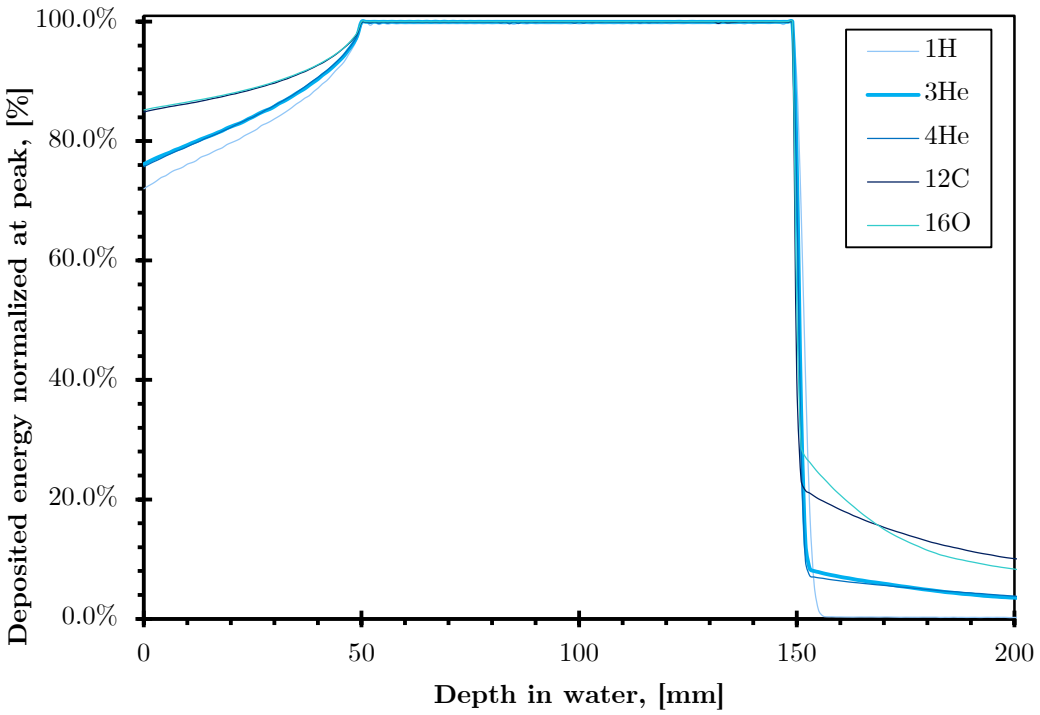

Figure 17. Physical dose optimized spread-out Bragg peak comparison for different ions: SOBP of 10 cm length with distal edge at 15 cm depth

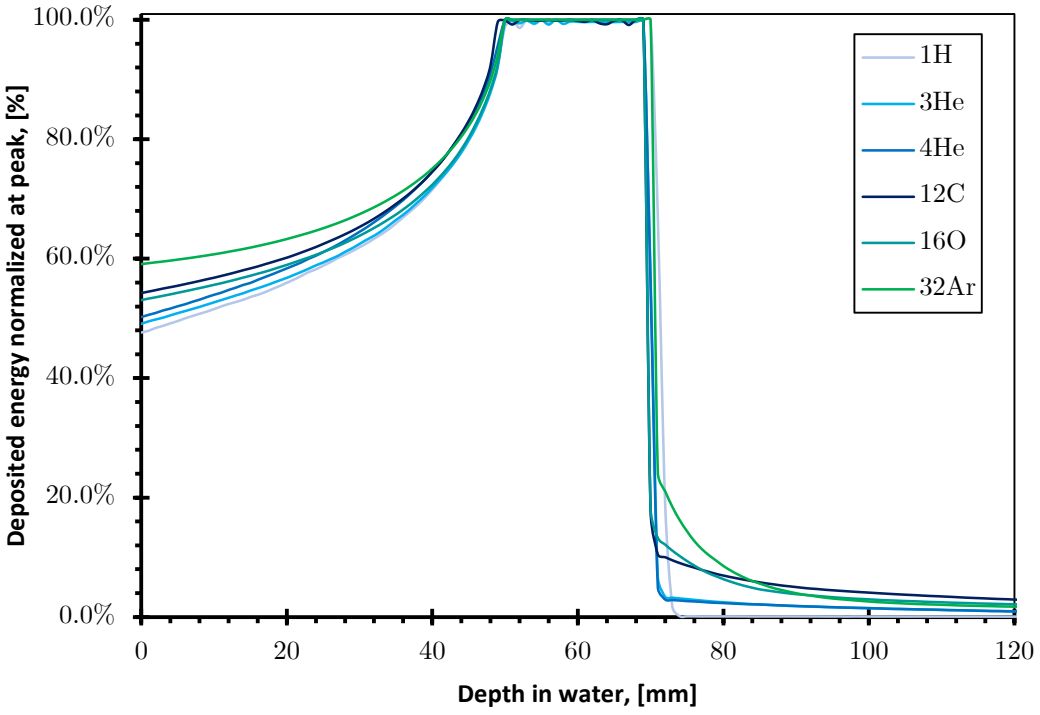

Figure 18. Physical dose optimized spread-out Bragg peak comparison for different ions: SOBP of 2 cm length with distal edge at 7 cm depth

Analyzing all of the visually represented data in figures 11. to 18. some of the main observations that can be drawn:

- by keeping the distal edge of SOBP at fixed depth and changing just the size/length of SOBP – entrance dose level decreases with decreasing SOBP length, clinically – decreasing tumor size.
- comparing SOBPs of same length with distal edge at 15 and 25 cm – for protons and helium ions entrance dose level is around the same for smaller SOBPs, but for larger SOBP of length 8 to 10 cm – the entrance dose level is higher if distal edge of SOBP is at 15 cm depth. For heavier ions – carbon and oxygen – the entrance dose level is around the same level or smaller for SOBP with distal edge at 15 cm depth.
- comparing different particle types, it can be visible that entrance dose increases with increasing atomic number of the particle – lowest physical entrance dose is seen in proton beam and increases for heavier particles. It must be noted that helium-3 and helium-4 ions have similar entrance dose level, but there are some noticeable differences. Entrance dose levels are almost equal for carbon and oxygen ions and Figure 18. shows that even for small and shallow SOBP it is already clearly visible that argon beams have the highest entrance dose level, when considering physical dose.
- considering differences primarily between just helium-3 and helium-4 ions, helium-3 ions have lower entrance dose level and in general lower dose levels proximal to peak region (the difference is in the range of 2 to 5%), that points to helium-3 ions being clinically more effective. As will be discussed in next point – on the downside helium-3 ions have higher tail dose level, but the difference is smaller than the beneficial difference in entrance region.
- when considering SOBP tail region, 2 main things should be pointed out:
    - although the difference is small (about 0.5%), helium-4 ions have lower fragmentation tail dose level than helium-3 ions right after peak region.
    - Figure 17. shows that tail region dose level is higher for oxygen ions in comparison with carbon ions right after the peak region, but after some distance beyond peak region oxygen ion tail region dose level drops below that for carbon ions. This indicates that secondary fragments of oxygen ion beams lose their energy faster than fragments of carbon ion beams. Figure 18. shows that when considering argon beams, although it has the highest initial tail dose level, it also decreases and at certain distance beyond peak region it becomes lower than the one for carbon beams.

- it should be also noted that proton SOBPs have more visible „ripples" in peak region than heavier particles (some can be visible on helium ion SOBPs as well). Although, it was not investigated in this study, the possible cause for this could be the step of pristine Bragg peaks in the set – if the optimization would have been done on a set with range increment step of 2 mm the effect of ripples could have been minimized and SOBP would be more uniform and homogenous. Optimization of SOBPs with different input pristine Bragg peak sets could reveal the necessary energy resolution needed to provide uniform dose distributions.

As discussed - main differences between physical dose optimized SOBPs for different ion types are entrance dose levels and fragmentation tail region dose levels. For quantitative estimation of the points made in previous discussion and dependence of these parameters on simulated treatment parameters (SOBP distal depth and length), from SOBPs energy deposition curves normalized at peak position these parameters were extracted:

- entrance to peak ratio, defining entrance at depth of 0 mm;
- tail to peak ratio at depth 1 cm beyond distal edge of SOBP;
- tail to peak ratio at depth 5 cm beyond distal edge of SOBP;

Values of these parameters are summarized in Tables 2. to 4. for all ion types considered in this study, except argon.

Table 2. Entrance to peak ratios for physical dose optimized SOBPs

SOBP length [cm]	Entrance to peak ratio (entrance dose) [%]									
	SOBP distal edge fixed at 25 cm (22 cm for ^{16}O) depth					SOBP distal edge fixed at 15 cm depth				
	^{1}H	^{3}He	^{4}He	^{12}C	^{16}O	^{1}H	^{3}He	^{4}He	^{12}C	^{16}O
10	62.2	68.7	69.3	87.9	86.6	72.0	76.2	75.7	84.9	85.2
9	60.1	66.7	67.5	86.1	84.6	68.8	73.1	72.7	82.3	82.6
8	57.8	64.4	65.6	84.0	82.5	65.4	70.0	69.6	79.4	79.7
7	55.3	62.2	63.3	81.5	79.7	61.8	66.6	66.3	76.5	76.6
6	52.6	59.7	61.1	78.7	76.8	58.2	63.0	62.8	72.8	73.1
5	49.0	56.6	58.1	75.4	73.6	54.1	59.0	59.1	68.8	69.1
4	45.8	52.7	54.8	71.4	69.4	49.7	54.6	54.7	64.6	64.5
3	41.8	48.0	50.4	66.8	64.2	44.4	49.3	49.7	58.5	58.8
2	36.4	42.4	45.0	60.7	57.7	38.0	42.7	43.6	51.4	51.8
1	29.3	34.2	37.2	50.0	48.7	29.6	33.7	34.5	42.3	42.2

Table 3. Tail to peak ratios 1 cm beyond peak for physical dose optimized SOBPs

SOBP length [cm]	Tail to peak ratio 1 cm beyond distal peak edge [%]									
	SOBP distal edge fixed at 25 cm (22 cm for ^{16}O) depth					SOBP distal edge fixed at 15 cm depth				
	^{1}H	^{3}He	^{4}He	^{12}C	^{16}O	^{1}H	^{3}He	^{4}He	^{12}C	^{16}O
10	0.7	12.1	10.9	30.3	31.8	0.3	7.0	6.4	18.3	20.7
9	0.7	12.1	10.8	30.1	31.7	0.3	7.0	6.4	18.3	20.7
8	0.7	12.0	10.7	29.9	31.6	0.3	7.0	6.3	18.2	20.7
7	0.7	11.8	10.6	29.5	31.4	0.3	7.0	6.3	18.4	20.6
6	0.7	11.7	10.5	29.2	31.2	0.3	6.9	6.2	17.9	20.4
5	0.5	11.4	10.2	28.7	31.0	0.3	6.8	6.1	17.7	20.3
4	0.6	11.1	9.8	28.0	30.5	0.3	6.6	5.9	17.6	20.0
3	0.6	10.5	9.3	26.9	29.8	0.3	6.3	5.6	16.6	19.5
2	0.5	9.6	8.5	25.2	28.5	0.2	5.9	5.2	15.5	18.8
1	0.5	8.2	7.3	21.4	25.5	0.2	4.9	4.3	13.7	17.0

Table 4. Tail to peak ratios 5 cm beyond peak for physical dose optimized SOBPs

SOBP length [cm]	Tail to peak ratio 5 cm beyond distal peak edge [%]									
	SOBP distal edge fixed at 25 cm (22 cm for ^{16}O) depth					SOBP distal edge fixed at 15 cm depth				
	^{1}H	^{3}He	^{4}He	^{12}C	^{16}O	^{1}H	^{3}He	^{4}He	^{12}C	^{16}O
10	0.4	7.7	7.8	21.1	13.9	0.2	3.5	3.8	10.1	8.3
9	0.4	7.7	7.7	20.9	13.9	0.2	3.5	3.8	10.1	8.3
8	0.4	7.6	7.7	20.8	13.8	0.2	3.5	3.8	10.0	8.3
7	0.4	7.5	7.6	20.5	13.6	0.2	3.5	3.8	10.2	8.2
6	0.4	7.4	7.5	20.2	13.4	0.2	3.5	3.7	9.9	8.1
5	0.3	7.2	7.3	19.8	13.2	0.2	3.4	3.7	9.7	8.0
4	0.3	7.0	7.0	19.2	12.8	0.2	3.3	3.6	9.6	7.7
3	0.3	6.6	6.7	18.4	12.2	0.2	3.1	3.4	8.9	7.4
2	0.3	6.1	6.1	17.2	11.4	0.2	2.9	3.2	8.2	6.8
1	0.2	5.2	5.2	14.6	10.0	0.2	2.4	2.6	7.1	5.9

Analyzing the data on entrance doses of SOBPs from Table 2.:

- for protons entrance dose is higher for shallower SOBPs (distal edge at 15 cm) than deap-seated SOBPs – around 10% higher for large SOBP (10 cm) decreasing to 1.5% for small SOBP (2 cm);
- for helium ions (both helium-3 and helium-4) entrance dose is higher for shallower SOBPs (distal edge at 15 cm) than deap-seated SOBPs, if SOBP is large – around 6 to 7% higher for large SOBP (10cm). If SOBP size is decreased to around to 4 to 3 cm – entrance dose levels are almost equal for shallow and deap-seated SOBPs. Decreasing SOBP size even further – entrance dose for shallower SOBPs is around 1 to 2 % lower than for deap-seated SOBPs.
- for carbon and oxygen ions entrance dose is lower for shallower SOBPs (distal edge at 15 cm) than deep-seated SOBPs:
    - for carbon ions difference of about 3% for SOBP of 10 cm inceases to a difference of about 8-9% for SOBP of 1 cm;
    - for oxygen ions difference of about 1.5% for SOBP of 10 cm inceases to a difference of about 6.5% for SOBP of 1 cm;
- for deap-seated SOBPs carbon ion entrance doses are about 1.5 – 2% higher than for oxygen ions for all SOBP sizes;
- for shallower SOBPs carbon and oxygen ion entrance doses are generally equal – the differenes are neglible not going higher than 0.5% for all SOBP sizes considered.

Analyzing the data on tail region dose levels of SOBPs from Tables 3. and 4. :

- for helium-3 and helium-4 ions - tail region dose level near peak region (1 cm) is around 1% higher for helium-3 ions, changing from 1.5% for large SOBPs to 0.5% for small SOBPs. Further away from peak region, tail region dose levels are almost equal for both helium ion types;
- for carbon and oxygen ions - tail region dose level near peak region (1 cm) is around 2-4% higher for oxygen ion than carbon. Further away from peak region, oxygen ion tail dose level decreases below carbon ion tail dose level – 4 to 7% for deep-seated SOBPs and around 1 to 2% for shallow SOBPs.

Lastly to analyze entrance doses, specifically the rate of entrance dose decrease with decreasing SOBP size, entrance dose values in each group (different particle, different SOBP distal edge depth) were normalized to the entrance dose value for corresponding 10 cm length SOBP. Visual representation of results is given in Figure 19.

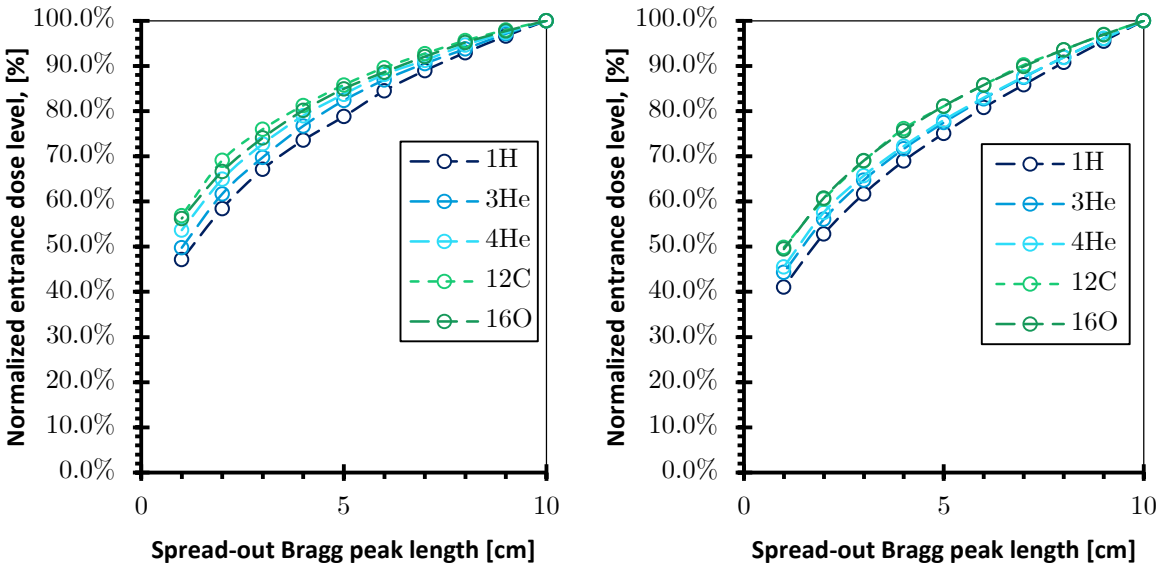

Figure 19. Physical dose optimized SOBP entrance dose dependence on SOBP length:

left SOBPs with distal edge at 25 (22) cm depth, *right* SOBPs with distal edge at 15 cm depth

From Figure 19. it is clearly observable:

- with decreasing SOBP length, entrance dose level decrease rate is more pronounced for shallower SOBPs;
- with decreasing SOBP length, entrance dose level decrease rate is largest for protons and rate of decrease gets a little lesser with increasing particle atomic number;
- decrease of entrance dose level is somewhat dependent on the value of SOBP length squared;

As was mentioned in the beggining of the study, one of the main factors impacting various ion type use for FLASH radiotherapy purposes is the compromise of the number of necessary particles for specific dose and number of particles that can be extracted in a single spill. For calculation of that firstly average deposited energy values were calculated at SOBP region. The data are given in Table 5.

Table 5. Average energy deposition in peak region of physical dose optimized SOBPs

SOBP length [cm]	Average energy deposit value at SOBP (MeV/mm)									
	SOBP distal edge fixed at 25 cm (22 cm for ^{16}O) depth					SOBP distal edge fixed at 15 cm depth				
	^{1}H	^{3}He	^{4}He	^{12}C	^{16}O	^{1}H	^{3}He	^{4}He	^{12}C	^{16}O
10	0.80	2.55	2.82	13.37	22.96	0.88	2.93	3.29	17.04	27.20
9	0.82	2.62	2.89	13.61	23.41	0.91	3.02	3.38	17.43	27.84
8	0.85	2.69	2.96	13.90	23.95	0.94	3.12	3.50	17.91	28.61
7	0.89	2.80	3.06	14.29	24.67	0.99	3.24	3.64	18.41	29.57
6	0.93	2.90	3.16	14.74	25.53	1.04	3.40	3.80	19.24	30.76
5	1.00	3.05	3.31	15.34	26.55	1.11	3.60	4.01	20.21	32.31
4	1.06	3.26	3.50	16.14	28.02	1.19	3.86	4.29	21.35	34.41
3	1.16	3.55	3.78	17.20	30.19	1.32	4.24	4.69	23.43	37.43
2	1.33	4.00	4.22	18.86	33.41	1.54	4.86	5.30	26.51	42.23
1	1.63	4.90	5.08	22.83	39.45	1.96	6.11	6.67	31.95	51.55

From data in Table 5 it must be noted that largest increase of deposited energy in SOBP region, when decreasing SOBP length from 10 to 1 cm, is for protons – around 2 times for deep-seated SOBP and 2.2 times for shallower SOBP. With increasingly heavier particles this deposited energy increment decreases and for oxygen ions it is 1.7 time increase for deep-seated SOBPs and 1.9 – for shallower SOBPs.

Having the data of deposited energy per milimetre in SOBP peak region, necessary number of particles was calculated to deliver uniform 2 Gy dose in SOBP uniform dose region. Irradiation volume was taken to be cubic – crossectional area dimensions were the same as corresponding SOBP length in depth direction. Calculations were done according to formula 2.5. and calculated data are given in Table 6. In Figure 20. a graphical representation is given.

Table 6. Calculated number of particles to deliver 2 Gy for cubic tumor in SOBP region

Tumor "size" [cm]	Number of particles to deliver 2 Gy at SOBP									
	SOBP distal edge fixed at 25 cm (22 cm for ^{16}O) depth					SOBP distal edge fixed at 15 cm depth				
	^{1}H	^{3}He	^{4}He	^{12}C	^{16}O	^{1}H	^{3}He	^{4}He	^{12}C	^{16}O
10	$1.6*10^{11}$	$4.9*10^{10}$	$4.4*10^{10}$	$9.3*10^{9}$	$5.4*10^{9}$	$1.4*10^{11}$	$4.3*10^{10}$	$3.8*10^{10}$	$7.3*10^{9}$	$4.6*10^{9}$
9	$1.2*10^{11}$	$3.9*10^{10}$	$3.5*10^{0}$	$7.4*10^{9}$	$4.3*10^{9}$	$1.1*10^{11}$	$3.4*10^{10}$	$3.0*10^{10}$	$5.8*10^{9}$	$3.6*10^{9}$
8	$9.4*10^{10}$	$3.0*10^{10}$	$2.7*10^{10}$	$5.7*10^{9}$	$3.3*10^{9}$	$8.5*10^{10}$	$2.6*10^{10}$	$2.3*10^{10}$	$4.5*10^{9}$	$2.8*10^{9}$
7	$6.9*10^{10}$	$2.2*10^{10}$	$2.0*10^{10}$	$4.3*10^{9}$	$2.5*10^{9}$	$6.2*10^{10}$	$1.9*10^{10}$	$1.7*10^{10}$	$3.3*10^{9}$	$2.1*10^{9}$
6	$4.8*10^{10}$	$1.5*10^{10}$	$1.4*10^{10}$	$3.0*10^{9}$	$1.8*1^{09}$	$4.3*10^{10}$	$1.3*10^{10}$	$1.2*10^{10}$	$2.3*10^{9}$	$1.5*10^{9}$
5	$3.1*10^{10}$	$1.0*10^{10}$	$9.4*10^{9}$	$2.0*10^{9}$	$1.2*10^{9}$	$2.8*10^{10}$	$8.7*10^{9}$	$7.8*10^{9}$	$1.5*10^{9}$	$9.7*10^{8}$
4	$1.9*10^{10}$	$6.1*10^{9}$	$5.7*10^{9}$	$1.2*10^{9}$	$7.1*10^{8}$	$1.7*10^{10}$	$5.2*10^{9}$	$4.7*10^{9}$	$9.4*10^{8}$	$5.8*10^{8}$
3	$9.7*10^{9}$	$3.2*10^{9}$	$3.0*10^{9}$	$6.5*10^{8}$	$3.7*10^{8}$	$8.5*10^{9}$	$2.7*10^{9}$	$2.4*10^{9}$	$4.8*10^{8}$	$3.0*10^{8}$
2	$3.8*10^{9}$	$1.2*10^{9}$	$1.2*10^{9}$	$2.6*10^{8}$	$1.5*10^{8}$	$3.3*10^{9}$	$1.0*10^{9}$	$9.4*10^{8}$	$1.2*10^{8}$	$1.2*10^{8}$
1	$7.6*10^{8}$	$2.5*10^{8}$	$2.5*10^{8}$	$5.5*10^{7}$	$3.2*10^{7}$	$6.4*10^{8}$	$2.0*10^{8}$	$1.9*10^{8}$	$3.9*10^{7}$	$2.4*10^{7}$

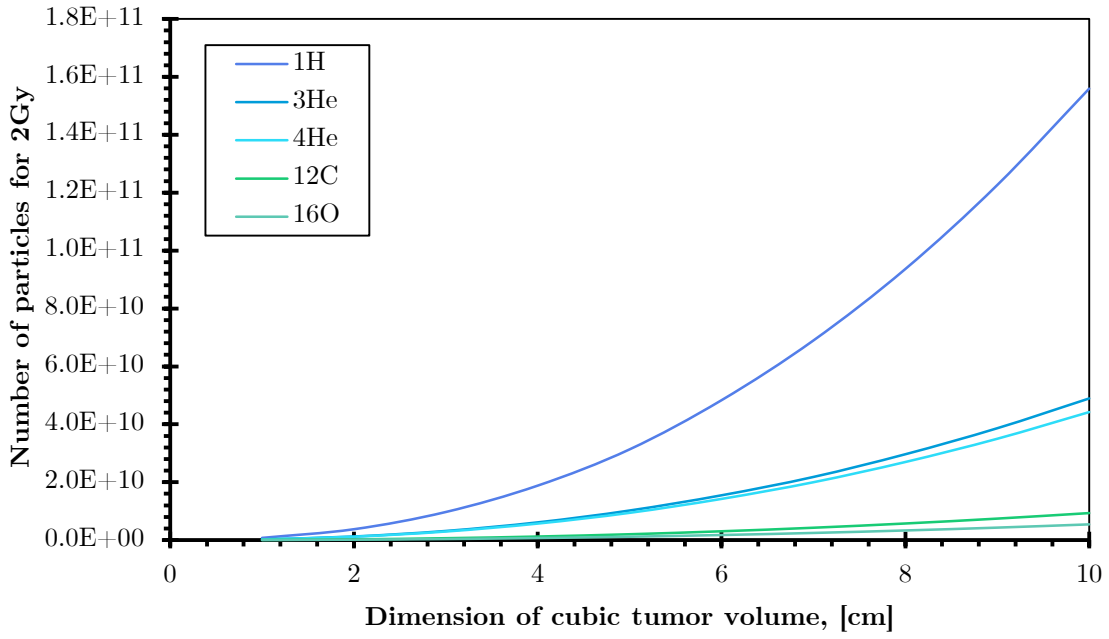

Figure 20. Number of particles simulated to deposit 2 Gy dose in deep seated (distal edge at 25 cm) cubic tumor volume

Analyzing the data:

- lesser number of particles is necessary to irradiate the same size SOBP (tumor) that is shallower compared to deep-seated tumors – around 10 to 20% less for protons and helium ions and 20 to 30% less for carbon and oxygen ions because of the increased energy deposition at shallower depths;
- helium ions require around 3 times less number of particles to deliver the same physical dose as protons, carbon ions – around 15 times less and oxygen ions – around 27 times less.
- calculated numbers of particles necessary to deliver 2 Gy for a specific volume are all within maximum number of particles per spill mentioned in 2.1. paragraph, indicating that such SOBPs could be deliverable using single spill of particles if muliple energy extraction is adequate.

3.3. Relative biological effectiveness and spread-out Bragg peaks based on biologically effective dose optimization

As was mentioned in 2.3. paragraph – for RBE value calculation with microdosimetric kinetic model, it is first necessary to calculate particle kinetic energy distribution and calculate the corresponding saturation-corrected dose-mean specific energy distributions. Going back to 2.3. paragraph – particle kinetic energy depth distribution was considered only for primary beam particles, ignoring secondary fragments and their energy deposition contributions (discussed in the next paragraph). In Figure 21. an example is given for calculated primary particle kinetic energy depth distribution of pristine Bragg peaks with range of 150 mm and corresponding depth distribution of saturation-corrected dose-mean specific energy.

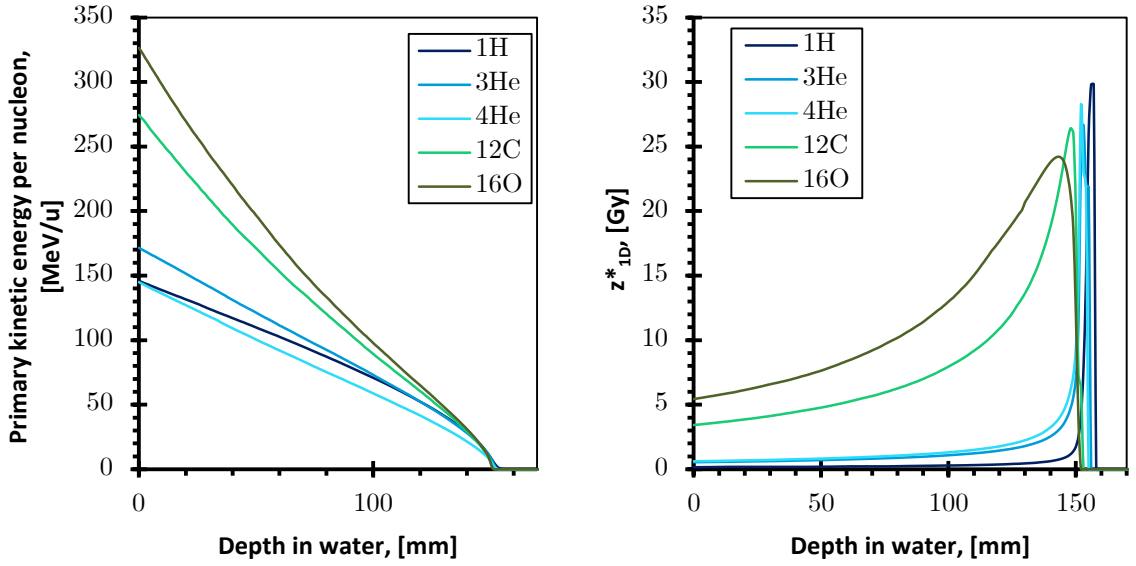

Figure 21. Example of simulation results of primary particle average kinetic energy depth distribution in water (*left*) and corresponding saturation-corrected dose-mean specific energy depth distribution (*right*)

Before going further, some observations of saturation-corrected dose-mean specific energy curves should be pointed out that will affect RBE curves:

- for protons – maximum value of z^*_{1D} happens to be after physical dose Bragg peak, meaning that proton biologically effective dose is more broadened in depth direction – biological dose range becomes larger than physical range;
- for helium ions – maximum value of z^*_{1D} happens to be around the same position as physical dose Bragg peak, creating the increase of biologically effective dose at SOBP distal edge.
- for carbon and oxygen ions - maximum value of z^*_{1D} happens to be before Bragg peak – shallower, meaning that the greatest biologically effective dose

increase coming from primary particles happens already in regions before Bragg peak. This aspect points in direction that secondary particle distributions and corresponding RBE values should be estimated as they could be the significant contributors of increased RBE exactly at Bragg peak position.

Continuing these calculations, biologically efffective dose calculations were first performed on physical SOBPs that already have an uniform physical dose distribution. In Figure 22. examples of calculated biologically effective dose distributions are given for 10 cm length SOBP that is physical dose optimized with distal edge at 25 cm depth for helium-4 and carbon ions.

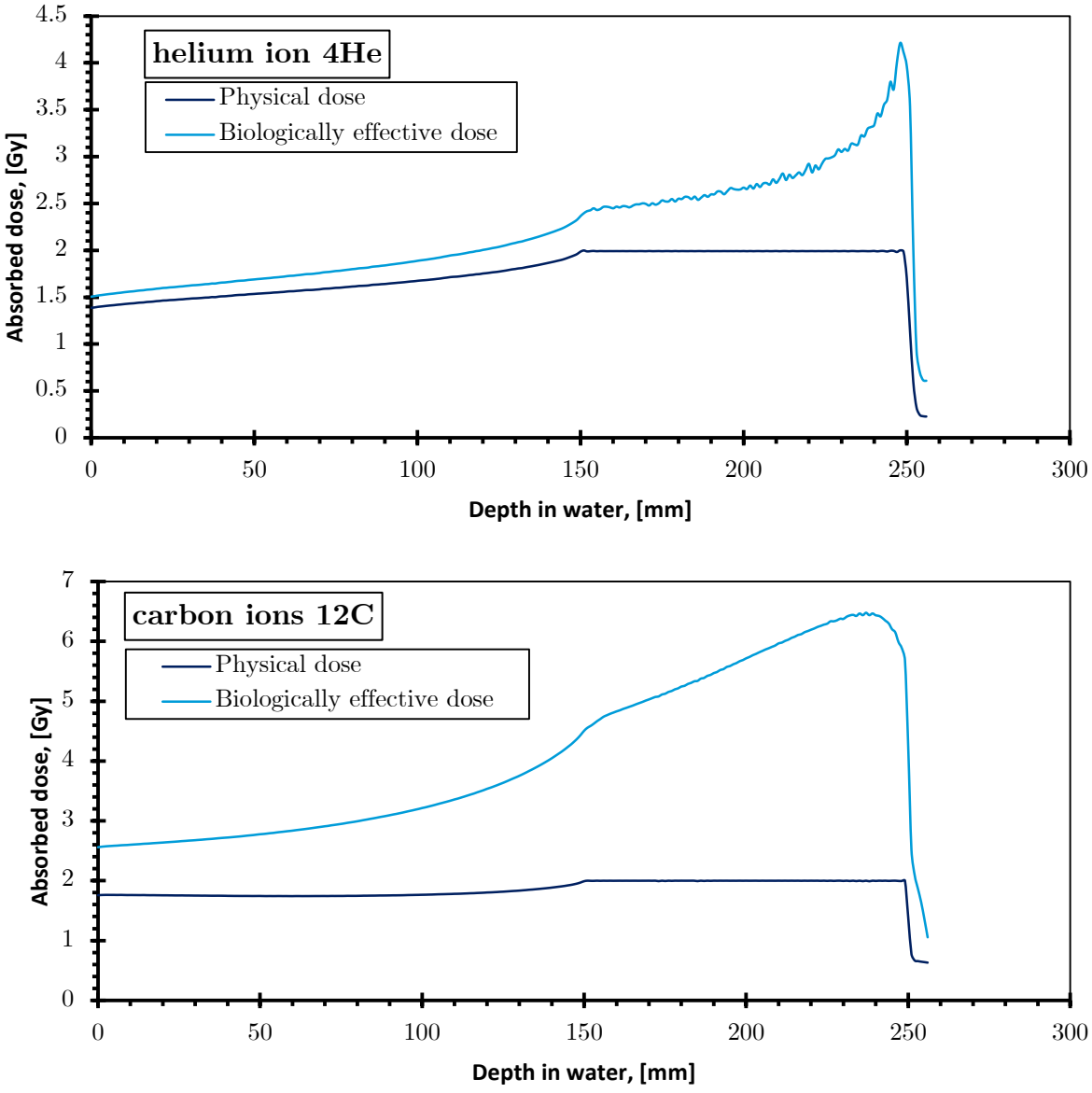

Figure 22. Example of resulting biologically effective dose distributions for physical dose optimized flat SOBPs

Based on results of Figure 22., it is clearly visible that a "flat" and uniform SOBP physical dose can not be used for treatment if biologically effective dose is considered, because such uniform physical dose distributions result in heavily non uniform and distally peaked biological dose distributions in tissue. Therefore the need for biologically optimized dose distributions is necessary if tissue irradiation is considered. Biologically effective dose SOBP optimization is done according to paragraph 2.4. To also estimate the impact of prescribed dose level on RBE values and therefore – physical dose distribution shape necessary to deliver uniform biologically effective dose SOBP, prescribed dose levels for biologically effective SOBP of 2, 5, 10 and 20 Gy were considered in SOBP biological optimization. In Figure 23. an example of physical dose depth distributions are given for the studied particle types to deliver uniform biologically effective SOBPs: 10 cm SOBP length with distal depth at 15 cm with prescribed dose level of 5 Gy.

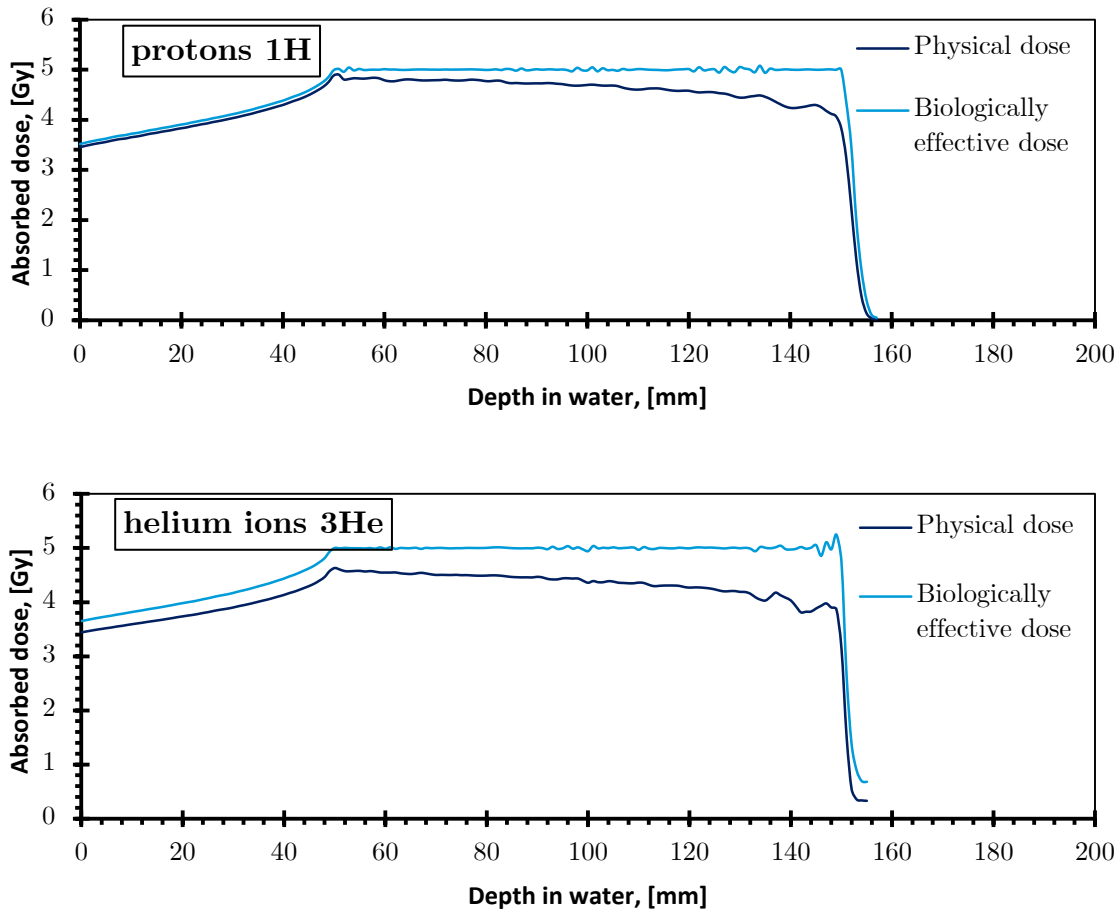

Figure 23. Biologically effective dose optimized SOBPs for 5 Gy prescribed dose and their corresponding physical dose distributions for studied particles

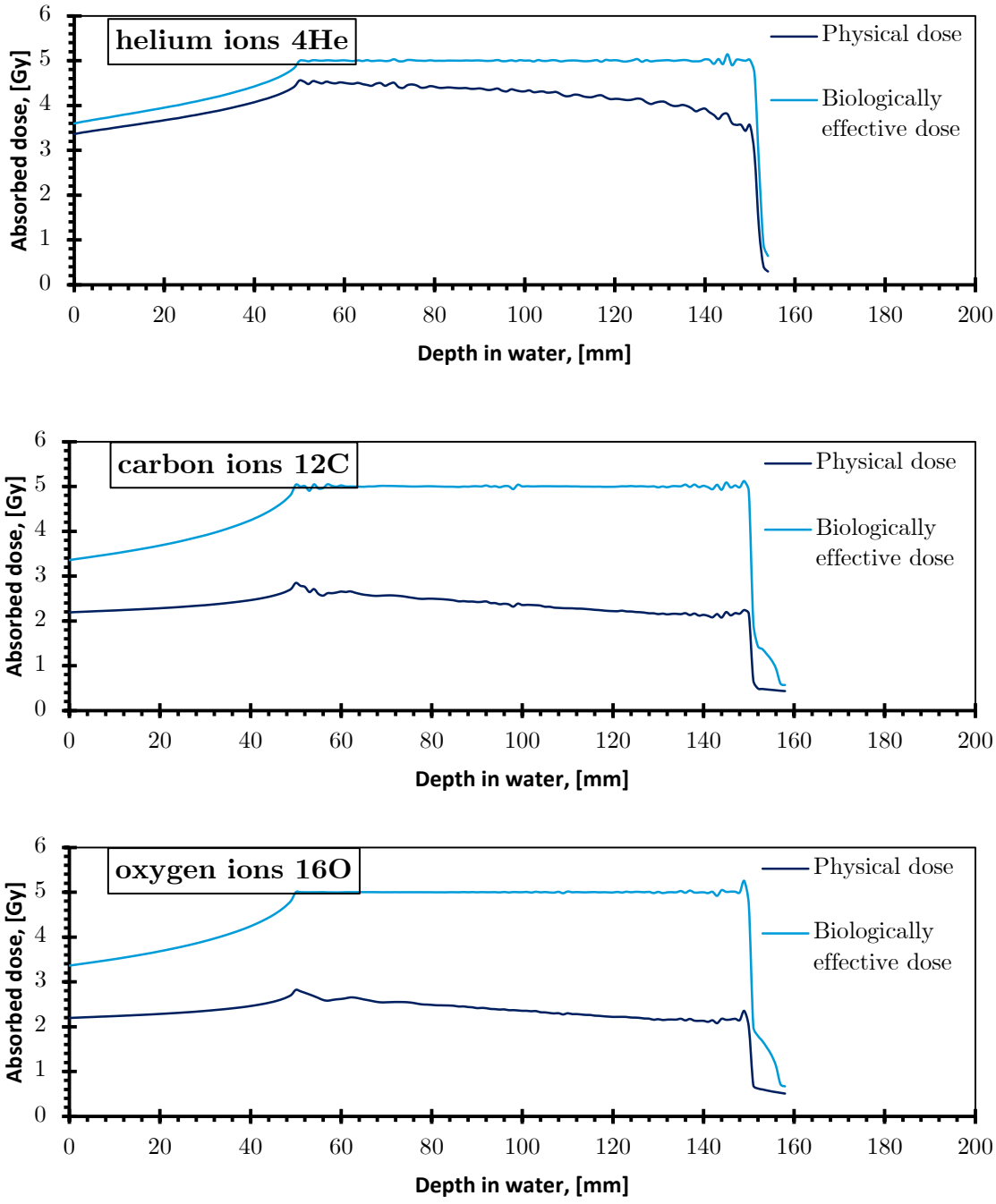

Figure 23. (cont.) Biologically effective dose optimized SOBPs for 5 Gy prescribed dose and their corresponding physical dose distributions for studied particles

Analyzing the data from Figure 23., it is clearly obsevable that:

- in order to obtain uniform and flat biologically effective dose SOBP, physical dose distribution is non-uniform – absorbed physical dose should decrease with increasing depth of SOBP, with minimum value at the distal edge of SOBP.

- in order to obtain certain dose level of biologically effective dose, physical dose can be lower because of the increased RBE value of heavy charged particles. Biologically effective dose increase is different in entrance region and peak region – RBE values are lower in the entrance region and higher in peak region, therefore making the biologically effective dose distribution more favorable – because of the biological effectiveness increase in peak region, entrance dose in relation to peak region becomes lower.
- entrance dose levels of biologically effective dose do not increase significantly from physical dose level for protons and helium ions, but for carbon and oxygen ions biologically effective dose increase even in entrance region is high. Going back to analysis of Figure 21. – it can clearly be seen that for heavy ions liks oxygen and carbon saturation-corrected dose-mean specific energy level is already high in entrance region leading to the increased RBE value.
- biological effectiveness parameter RBE increases for heavier ions like carbon and oxygen – in comparison to protons or light ions (helium) lower physical dose levels are necessary to obtain the same biologically effective dose level.
- for protons and helium ions it can be seen that biologically effective dose has increased range in tissue in comparison to physical dose – as was mentioned with analysis of Figure 21. – proton RBE is maximum beyond the distal edge of Bragg peak, therefore biologically effective range broadening is present and must be carefully taken into account of clinical treatment planning.

For further analysis on biologically effective dose optimized SOBPs data regarding peak region prescribed dose level impact on necessary physical dose distribution are given as examples in Figures 24. and 25. :

- Figure 24. gives visual representation in changes of necessary physical dose distributions to achieve uniform biologically effective dose in SOBP region for various prescribed dose levels for deep-seated (distal edge at 250 mm) SOBP of 10 cm length. For comparison purposes physical dose distributions for various dose levels are normalized at entrance (d = 0 mm), only example is given for helium-4 ions, althought the trend visible in Figure 24. is present for different particle types as well.
- Figure 25. gives biologically effective dose optimized deep-seated SOBPs for various prescribed dose levels, SOBP length – 5 cm. For comparison purposes SOBPs are normalized at peak region – to prescribed dose level. Data is given for protons, helium-4 and carbon ions, because helium-3 ions have the same trend of prescribed dose level impact as helium-4 ions, but oxygen ions – the same trend as carbon ions.

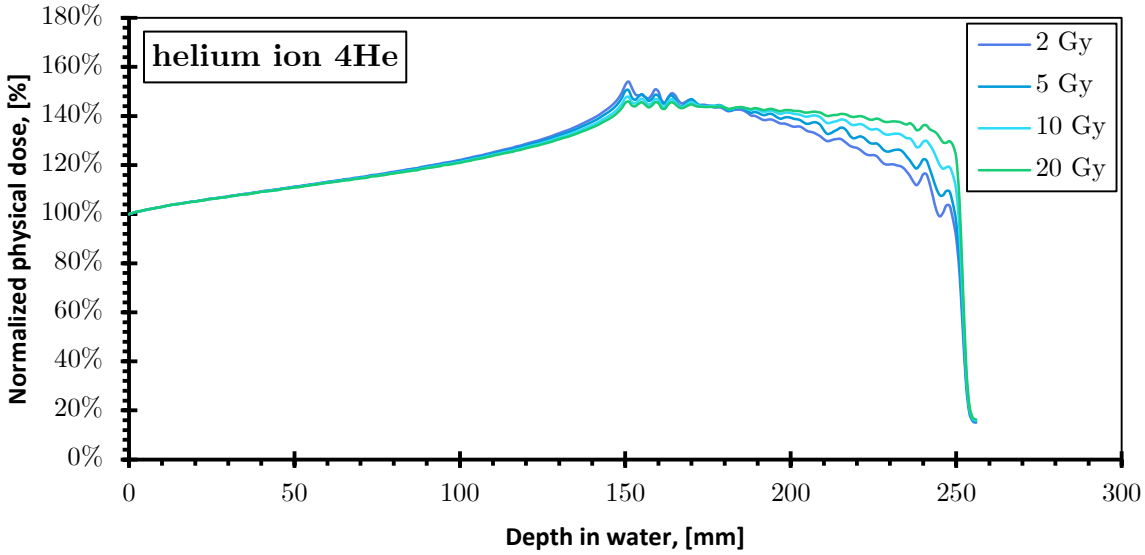

Figure 24. Example of physical dose distributions for biologically effective dose optimized SOBPs for different dose levels in peak region for helium-4 ions

Analyzing data in Figure 24., it can be seen that with increasing prescribed dose level at SOBP the necessary physical dose distribution to achieve uniform biologically effective dose becomes less ramp-like and approached uniformity already in physical dose domain. The reason for this comes from the theory given in 2.4. paragraph of charged particle relative biological effectiveness in tissue – RBE values for the same cell type and same radiation characteristics decrease as function of dose, therefor RBE is maximal for lower dose levels. This way RBE value's peak at the distal edge of SOBP decreases with increasing prescribed dose and therefore – physical dose distribution necessary becomes more close to uniform one. This aspect on necessary physical dose distribution characteristics dependence on prescribed biologically effective dose level makes an impact on calculations of number of particles necessary for particular dose level and is later discussed in this paragraph.

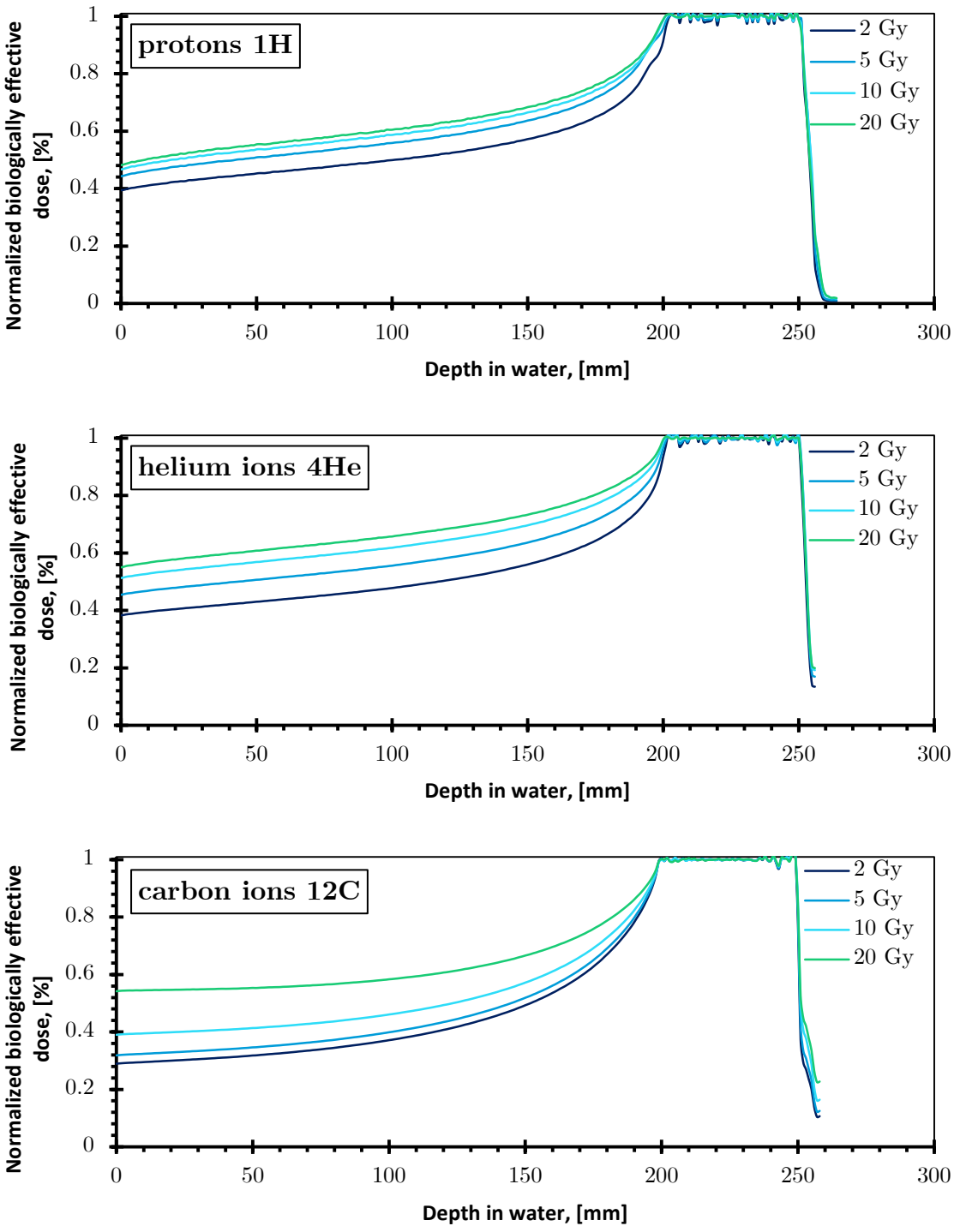

Figure 25. Relative dose deposition curves for biologically effective SOBP's for different dose levels and different studied particles

Analyzing the data given in Figure 25. for deep-seated tumors:

- it can be seen that with increasing prescribed dose level at SOBP entrance dose level in comparison to peak region also increases – lowest entrance dose levels can be seen for 2 Gy prescribed dose. This comes from the RBE dependence on dose – with increasing dose RBE values deacrease, therefore the beneficial difference between entrance region RBE and peak region RBE becomes smaller.
- prescribed dose level impact on changes in entrance dose level becomes more pronounced in heavier ions – while for protons, increasing peak prescribed dose level from 2 to 20 Gy, the change in relative entrance dose level is about 9%, while for helium ions it is around 17% and for carbon ions – 22%.
- for the same dose level, entrance relative doses are higher for helium-4 ions than protons. As it was discussed already in previous paragraph – physical dose entrance level is already higher for helium ions, so it can be seen that RBE value difference in peak and entrance regions is not enough in case of helium-4 ions, therefore by entrance dose parameters helium ions seems less effective than protons.
- for the same dose level, entrance relative doses are lower for carbon ions in comparison to protons and helium ions, if the prescribed dose level is 10 Gy or lower. These beneficial characteristics of carbon ions come from the fact, that difference in RBE values in peak and entrance regions for carbon ions is large enough to overcome the physically increased entrance dose as seen in previous chapter. Although, it is also noticable that for prescribed dose level of 20 Gy, relative entrance dose of carbon ions is larger than protons and approaches the same level as helium ions.

For further quantitative analysis of entrance dose relative level changes, entrance doses were calculated for all biologically effective dose optimized SOBPs – in Table 7. data are given regarding deep-seated SOBPs for both SOBP lengths, but for shallower SOBPs – in Table 8. For more easily observable results, visual representation of data is also given in Figure 26. It must be noted, that for deep-seated SOBPs data for oxygen ions are not included because the output data of optimization were noisy for this particular case.

Table 7. Entrance to peak ratios (entrance doses) for biologically effective dose optimized SOBPs with distal edge at 25 cm depth at various dose levels

Biologically effective dose (Gy)	Biologically effective entrance dose level (%)							
	10 cm SOBP length				5 cm SOBP length			
	^{1}H	^{3}He	^{4}He	^{12}C	^{1}H	^{3}He	^{4}He	^{12}C
2	55.8	57.5	56.5	45.2	39.4	38.9	38.3	28.9
5	59.1	62.7	62.1	50.0	44.3	45.7	45.5	31.9
10	60.6	65.7	65.6	60.3	46.7	50.5	51.3	39.0
20	61.5	67.4	67.6	73.1	48.2	53.7	55.0	54.2

Table 8. Entrance to peak ratios (entrance doses) for biologically effective dose optimized SOBPs with distal edge at 15 cm depth at various dose levels

Biologically effective dose (Gy)	Biologically effective entrance dose level (%)									
	10 cm SOBP length					5 cm SOBP length				
	^{1}H	^{3}He	^{4}He	^{12}C	^{16}O	^{1}H	^{3}He	^{4}He	^{12}C	^{16}O
2	68.4	70.1	68.7	62.2	62.3	46.2	47.2	45.6	36.9	37.1
5	70.3	73.0	72.0	67.2	67.3	50.1	52.3	51.5	41.1	41.3
10	71.2	74.6	73.8	73.8	74.0	52.2	55.5	55.1	49.0	49.2
20	71.7	75.5	74.8	79.3	79.6	53.4	57.3	57.3	58.7	58.9

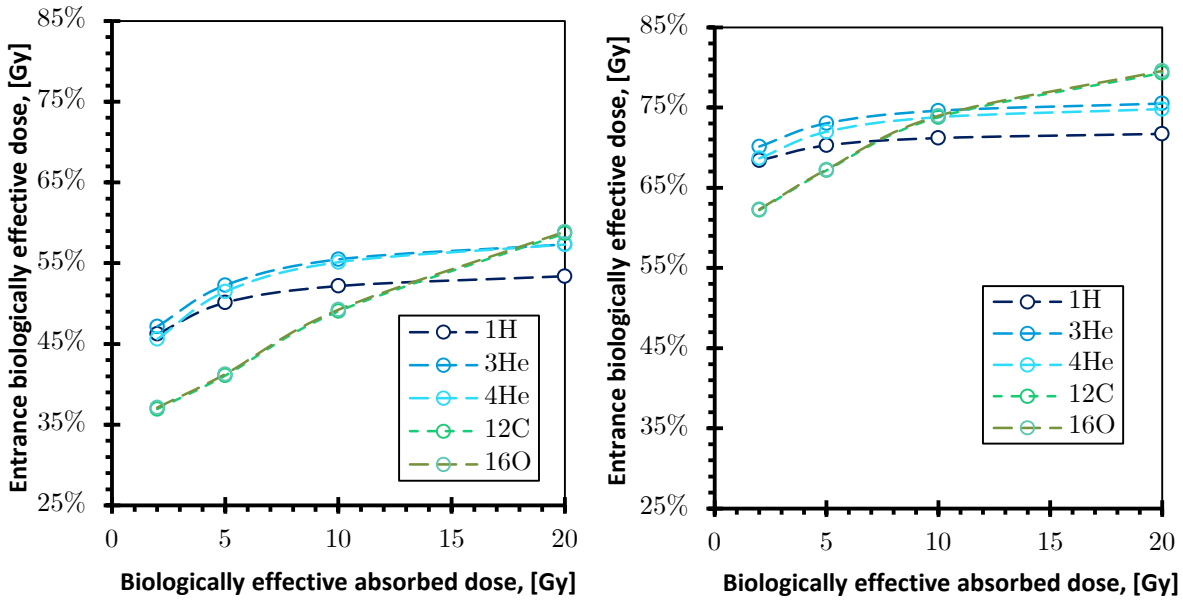

Figure 26. Biologically effective absorbed dose optimized SOBP entrance dose dependence on effective absorbed dose level for shallower SOBPs

left SOBP of 5 cm length, *right* SOBP of 10 cm length

From quantitative data given in Table 7. and Table 8., the previous analysis can be expanded:

- for the same dose level, helium ions have entrace dose relative levels higher or around the same value as protons for both deep-seated and shallower SOBPs and for both SOBP sizes. It can only be seen in deep-seated, 5 cm SOBP case with prescribed dose level of 2 Gy – helium ion entrance dose level is about 0.5% lower than protons.
- for carbon (the same applies for oxygen ions) ions this dependence is more complex:
    - for deeply-seated SOBPs, carbons ions have lower entrance dose than protons for doses below 10 Gy for SOBP length of 5 cm, but if SOBP length is 10 cm – carbon ion entrance dose is lower for doses below 5 Gy, at 10 Gy prescribed dose – entrance dose is equal with protons. For 20 Gy prescription dose – carbon ion entrance dose is higher in both cases.
    - for shallower SOBPs, the same trend is present as for deeply-seated tumors, except for 10 cm SOBP length – entrance dose for carbon ions is already higher than proton case.
- the magnitude of carbon ion biological dose „benefit" over protons is also dependent on SOBP depth and SOBP length as for deep-seated SOBPs maximum decrease of entrance dose for both SOBP lengths is about 10%, while in case of shallower SOBPs – for 10 cm SOBP it is about 5%, while for 5 cm SOBP – about 10%.
- from Figure 26. it appears that entrance dose for protons and heliums ions in dependence of prescribed dose level follows logarithmic function like trend, while for carbon and oxygen ions – the trend of dependence appears to be almost linear.

For confirmation of trends observed and further quantitative analysis on biological effectiveness of each particle type studied, RBE values were extracted from each of the biologicallly effective dose optimized SOBPs. RBE values of each SOBP were extracted at the 3 positions on dose deposition curve – entrance depth (0 mm), depth of SOBP middle and at depth 1mm proximal to the distal edge of SOBP. Collected data for deap-seated SOBPs are presented in Table 9., but for shallower SOBPs – in Table 10.

Table 9. Relative biological effectiveness for biologically effective dose optimized SOBPs with distal edge at 25 cm depth at various dose levels and different SOBP regions

Biologically effective dose (Gy)	10 cm SOBP length				5 cm SOBP length			
	^{1}H	^{3}He	^{4}He	^{12}C	^{1}H	^{3}He	^{4}He	^{12}C
	RBE value at beam entrance							
2	1.03	1.09	1.10	1.69	1.03	1.09	1.11	1.72
5	1.02	1.05	1.06	1.47	1.02	1.06	1.07	1.56
10	1.01	1.03	1.03	1.24	1.01	1.03	1.04	1.34
20	1.01	1.02	1.02	1.10	1.01	1.02	1.02	1.13
	RBE value at middle of SOBP							
2	1.19	1.37	1.42	3.52	1.41	1.68	1.81	4.71
5	1.09	1.20	1.22	2.78	1.19	1.39	1.44	3.89
10	1.05	1.10	1.12	1.93	1.13	1.19	1.22	2.72
20	1.03	1.05	1.06	1.38	1.05	1.09	1.10	1.64
	RBE value at distal edge of SOBP							
2	1.60	1.68	1.82	3.63	1.65	2.12	2.13	4.55
5	1.34	1.43	1.54	2.87	1.34	1.66	1.76	3.74
10	1.19	1.24	1.32	1.99	1.22	1.32	1.42	2.60
20	1.10	1.12	1.16	1.42	1.11	1.15	1.20	1.60

Table 10. Relative biological effectiveness for biologically effective dose optimized SOBPs with distal edge at 15 cm depth at various dose levels and different SOBP regions

Biologically effective dose (Gy)	10 cm SOBP length					5 cm SOBP length				
	^{1}H	^{3}He	^{4}He	^{12}C	^{16}O	^{1}H	^{3}He	^{4}He	^{12}C	^{16}O
	RBE value at beam entrance									
2	1.03	1.11	1.12	1.84	1.84	1.03	1.12	1.13	1.87	1.87
5	1.02	1.06	1.07	1.53	1.53	1.02	1.07	1.08	1.65	1.65
10	1.01	1.03	1.04	1.27	1.27	1.01	1.04	1.05	1.37	1.36
20	1.01	1.02	1.02	1.12	1.12	1.01	1.02	1.03	1.16	1.16
	RBE value at middle of SOBP									
2	1.12	1.25	1.29	2.75	2.75	1.29	1.46	1.54	3.67	3.65
5	1.06	1.13	1.16	2.12	2.12	1.14	1.25	1.29	2.91	2.88
10	1.03	1.07	1.08	1.57	1.57	1.07	1.13	1.15	2.01	2.00
20	1.02	1.04	1.04	1.25	1.25	1.04	1.06	1.07	1.41	1.41
	RBE value at distal edge of SOBP									
2	1.49	1.64	1.63	2.97	2.91	1.45	1.70	1.93	3.68	3.64
5	1.23	1.36	1.46	2.28	2.23	1.31	1.51	1.60	2.91	2.86
10	1.12	1.20	1.27	1.67	1.63	1.16	1.26	1.34	2.00	1.97
20	1.06	1.10	1.14	1.30	1.28	1.08	1.13	1.18	1.41	1.38

Analyzing the data from Table 9. and Table 10.:

- RBE values at entrance region are independent of SOBP length or depth as they do not change significantly between these different cases for all studied particle types, except for carbon and oxygen ions – RBE values at entrance region are the same for different SOBP length, but for shallower SOBPs it increases from around 1.7 to 1.85.
- RBE values at the region of SOBP middle are dependent both on SOBP length and depth:
    - for larger SOBP length, RBE values are smaller – for protons and helium ions the difference is about 20% at 2 Gy dose and 2 % at 20 Gy dose, while for carbon and oxygen ions – 30% at 2 Gy and 10 % at 20 Gy level.
    - for deep-seated SOBPs RBE values are larger than shallower SOBPs - for protons and helium ions the difference is about 10-15% at 2 Gy dose

and 2 % at 20 Gy dose, while for carbon and oxygen ions – 30% at 2 Gy and 1-15 % at 20 Gy level.

- RBE values at the distal edge of SOBP are dependent both on SOBP length and depth and the trends of dependence are similar like for RBE values at SOBP middle region.
- difference between entrance region and peak region RBE values is the largest for carbon and oxygen ions, leading to the increased difference between peak and entrance dose discussed in previous parts.

Last consideration regarding biologically effective dose optimized SOBPs were calculating the number of particles necessary for their respective physical dose distributions. Physical dose distributions of each of the biologically effective dose optimized SOBPs were taken together with the respective distributions of particle energy deposition. Taking physical dose value and the respective energy deposition value from the distributions at certain depth (was chosen at 0 mm depth, this has no effect on calculation result), number of particles to achieve physical dose to a coressponding biologically effective dose optimized SOBP was calculated according to formula 2.5. Dosed were calculated to cubic shaped volumes of 10x10x10 and 5x5x5 cm, corresponding to two SOBP lengths considered in this part of study. Calculations were done at each of the biologically effective dose levels considered. For comparison values from Table 6. were taken and recalculated for each dose level to consider the impact biological effectiveness – ratios were calculated between number of particles necessary to achieve a uniform certain biologically effective dose level and the number of particles to achieve the same dose level in physical dose domain, neglecting all of biological effect. Calculated ratios are given in Table 11. for deep-seated SOBPs and in Table 12. for shallower SOBPs.

Table 11. Ratios between necessary number of particles for biologically effective dose level and the same value physical dose level for SOBPs with distal edge at 25 cm depth

	number of particles for biologically effective dose / number of particle for physical dose							
Absorbed dose (Gy)	Tumor of 10x10x10 cm				Tumor of 5x5x5 cm			
	^{1}H	^{3}He	^{4}He	^{12}C	^{1}H	^{3}He	^{4}He	^{12}C
2	0.86	0.76	0.73	0.30	0.78	0.62	0.59	0.22
5	0.93	0.86	0.84	0.38	0.88	0.76	0.73	0.27
10	0.96	0.92	0.91	0.55	0.94	0.86	0.85	0.39
20	0.98	0.96	0.96	0.75	0.98	0.93	0.93	0.63

Table 12. Ratios between necessary number of particles for biologically effective dose level and the same value physical dose level for SOBPs with distal edge at 15 cm depth

	number of particles for biologically effective dose / number of particle for physical dose									
Absorbed dose (Gy)	Tumor of 10x10x10 cm					Tumor of 5x5x5 cm				
	^{1}H	^{3}He	^{4}He	^{12}C	^{16}O	^{1}H	^{3}He	^{4}He	^{12}C	^{16}O
2	0.91	0.82	0.79	0.39	0.39	0.82	0.71	0.68	0.29	0.29
5	0.95	0.89	0.88	0.50	0.50	0.90	0.82	0.80	0.36	0.36
10	0.97	0.94	0.93	0.67	0.67	0.95	0.90	0.89	0.52	0.52
20	0.99	0.97	0.97	0.82	0.82	0.98	0.95	0.95	0.74	0.73

Analyzing the data from Table 11. and Table 12.:

- if biological effects of dose deposition in living cells are taken into account, then always a smaller number of particles is necessary to deliver the same physical dose level as biologically effective dose;
- ratios generally follow the trends that are observable with RBE values – ratios are smaller for heavier particles (more efficiency), ratios increase with increasing dose (less efficiency) and ratios are dependent on SOBP length and depth, showing more efficiency for smaller SOBP lengths and deeper seated SOBPs.

- if the biological effectiveness is considered, number of necesserary particles for certain dose loses the linear dependence on dose level. For example, in Figure 28. the relationship of number of particles neccessary and dose level is given in both physical and biologically effective dose domains for carbon ions irradiating a 5x5x5 cm volume with distal edge at 250 mm depth.

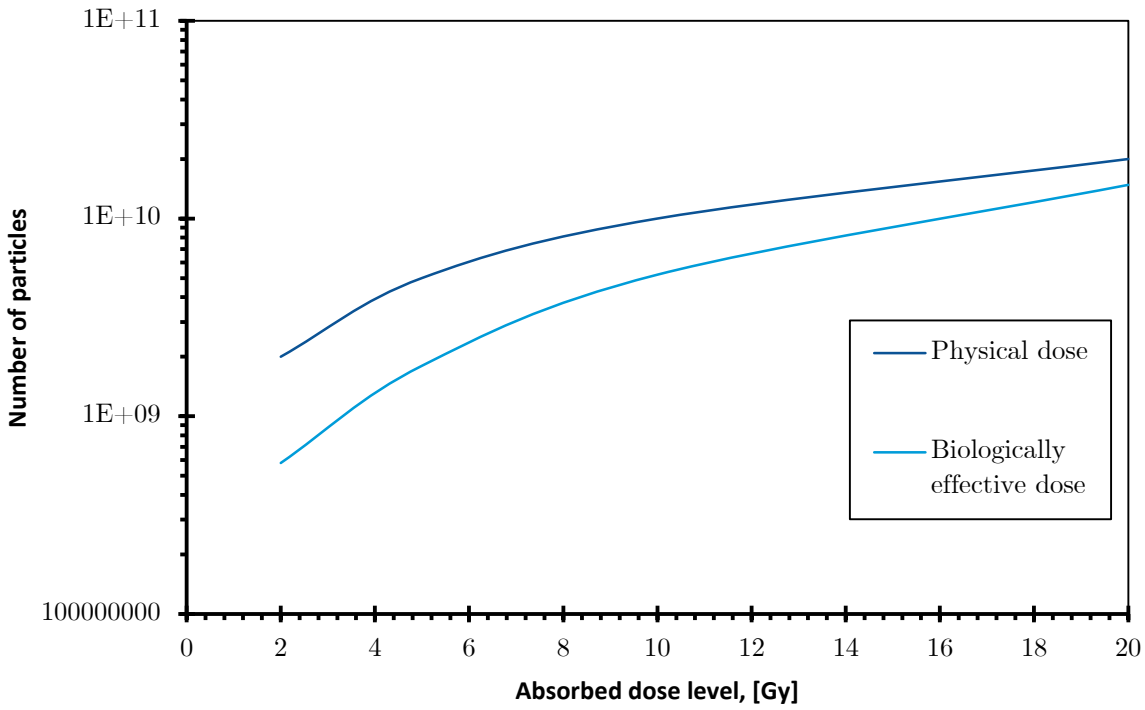

Figure 27. Number of particles in dependence of absorbed dose level for physical and biologically effective doses

3.4. Relative biological effectiveness calculation issues in regards to secondary particle "contamination"

As was stated in Method paragraph, for biological effectiveness studies only primary particles were considered for RBE calculation and no secondary particles – beam fragments – were taken into account. This last paragraph focuses on this aspect and gives estimates on possible impact of this.

It is known that for heavier charged particles secondary fragments of lighter particles are present in radiation field and these secondary fragments, having lighter mass, extend beyond the Bragg peak of primary particles creating fragmentation tail dose. Even for protons, secondary particles are present in the beam – recoil protons, but only neglible energy deposition extension beyond Bragg peak is observable for proton beams. What is more, secondary particle generation intensity also depends on the material irradiated – in radiotherapy aspect it would depend on tissue type irradiated as irradiatin dense bone would provide more secondary particles and possibly with higher atomic number than initial primary particle.

As seen in Figure 2. in paragraph 2.3 - saturation-corrected dose-mean specific energy values that are the main input data for RBE calculation with microdosimetric kinetic model heavily depend on the atomic number of the particle. As seen in Figure 21. in paragraph 3.3. it is shown that because of this reason the actual specific energy depth distribution heavily differs for various particle types: for lighter particles being more peaked and for heavier ones – more broadened. Because of this reason secondary beam fragments do affect the shape of RBE curve in depth as the secondary particles for heavier ions could give rise to more peaked RBE at distal edge of SOBP.

To estimate the impact of secondary particles on RBE values, secondary particle contributions to total energy deposition were estimated for pristine Bragg peaks. Monte Carlo simulations were run in Geant4 to calculate total energy deposition (taken from 3.1. paragraph), primary particle energy deposition and also primary particle fluence was simulated with custom made Geant4 code based on Hadr01 example. Secondary particle energy deposition was calculated by subtracting primary particle energy deposition curve from the total energy deposition curve. In Figure 28. energy deposition curves from primary and secondary particles are given for pristine Bragg peaks with range of 150 mm. In Figure 29. energy deposition of secondary particles is given as fraction of total energy deposition for pristine Bragg peaks with range of 150 and 250 mm, but in Figure 30. – primary particle fluence is given for pristine Bragg peaks with range of 150 and 250 mm.

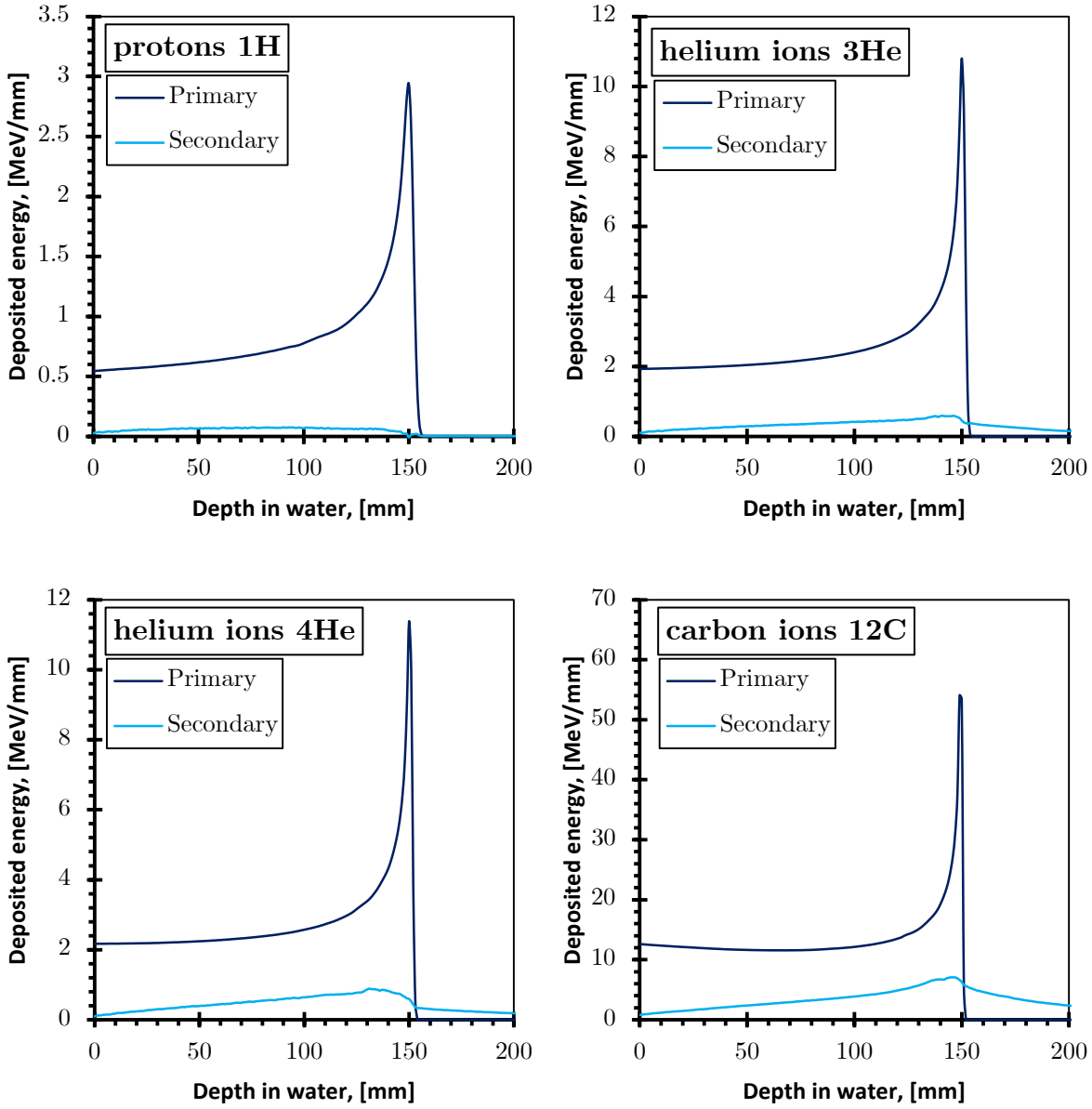

Figure 28. Primary particle and secondary fragment energy deposition depth curves for pristine Bragg peaks with range of 150 mm.

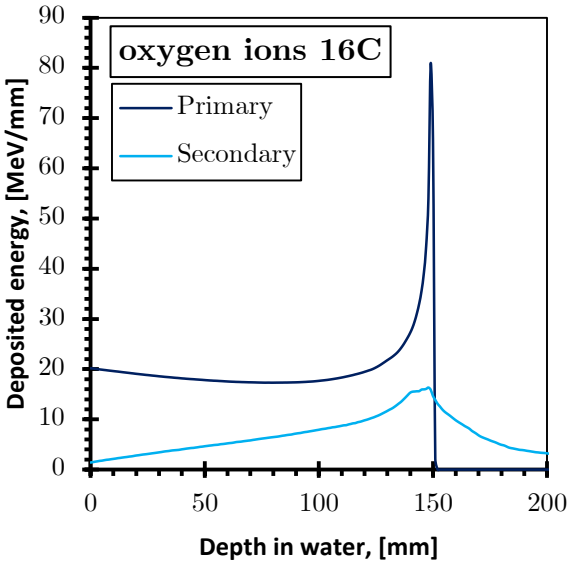

Figure 28. (cont.) Primary particle and secondary fragment energy deposition depth curves for pristine Bragg peaks with range of 150 mm.

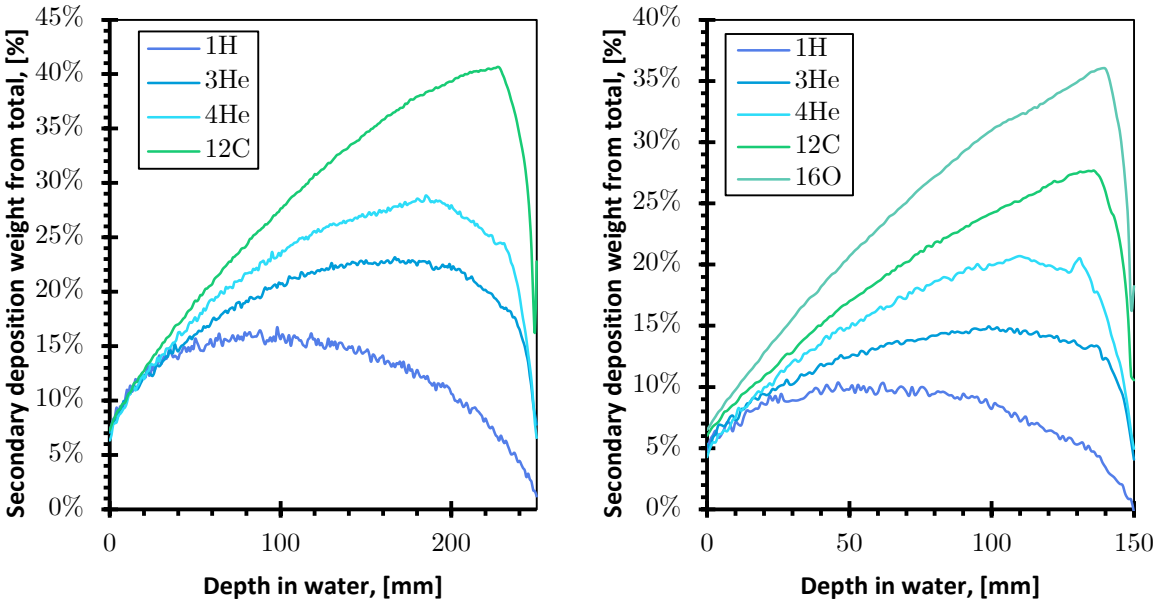

Figure 29. Secondary fragment energy deposition as fraction of total energy deposition in dependence of depth:

left for pristine peaks with range of 250 mm, *right* for pristine peaks with range of 150 mm

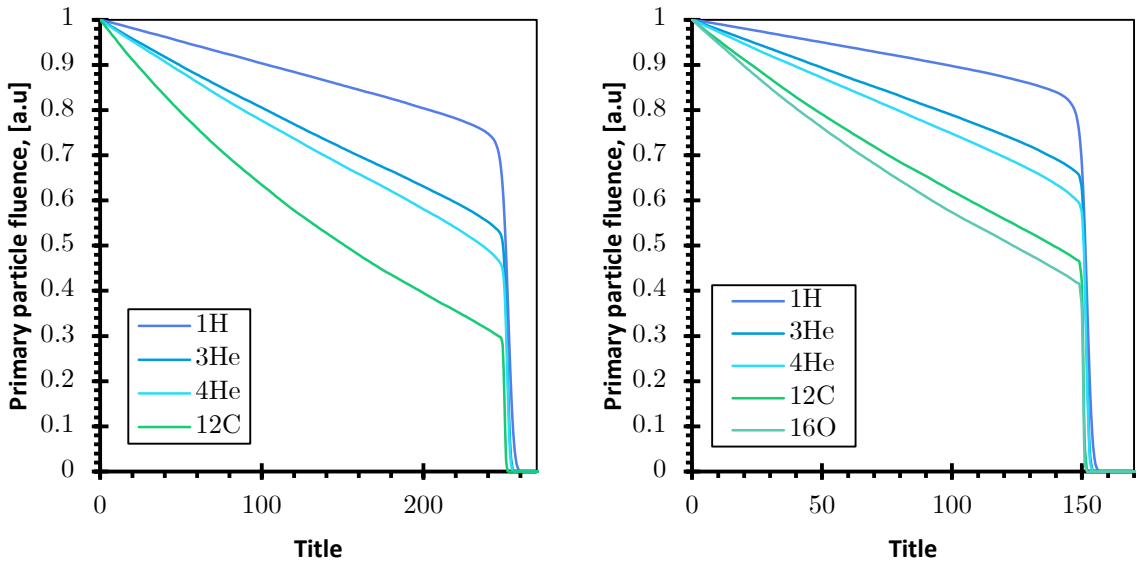

Figure 30. Primary particle fluence loss in dependence of depth:

left for pristine peaks with range of 250 mm, *right* for pristine peaks with range of 150 mm

Analyzing the data from Figures 28. to 30.:

- energy deposition from secondary particles increases with depth and peaks at certain depth – for protons this deposition maximum happens around the middle of Bragg peak range, but for heavier ions – closer to Bragg peak of primary particles. Energy deposition maximum of secondary particles moves closer to Bragg peak of primary particles with increasing particle mass.
- at the Bragg peak energy deposition of secondary particles decreases from the maximum value of secondary energy deposition, but this heavily depends on particle type: for pristine Bragg peak ranges considered here - for protons secondary particles contribute less than 1% of energy deposition at Bragg peak, for helium-3 and helium-4 ions 5-7%, for carbon ions – 11-16% and oxygen ions – around 16%. This shows that the maximum impact on RBE calculations around Bragg peak region and therefore distal end of SOBP can be seen for carbon and oxygen ions, as for protons it would neglible and helium ions – small, but still significant.
- with increasing range of pristine Bragg peaks secondary particle contribution to total energy deposition increases – as particles traverse more absorber material and initial energy, more nuclear fragmentation processes happen. Increasing pristine Bragg peak range from 150 to 250 mm, maximum secondary particle contribution to total energy deposition increases of about 5% for protons and around 13% for carbon ions. This effect also points to a

fact that the impact of secondary particles is more pronounced for deeply-seated tumors and therefore RBE calculation for deep SOBPs is more dependent on secondary lighter particles.

- although clearly understandable, it must be noted that secondary particle contribution to RBE calculations needs to be taken into account in regards to tail region beyond the Bragg peak as no primary particles are present. It is og high importance in clinical dosimetry to check that elevated RBE levels are not placed in areas of critical organs beyond Bragg peak to avoid possible damage and complications after treatment.
- as can be seen in Figure 30. primary particle decreases with increasing depth and abruptly drops to zero at the end of the range. It is also visible that the rate of fluence decrease becomes larger for heavier particles, indicating the previous stated point – heavier charged particles undergo more nuclear interactions in absorber material. As primary particle fluence decreases dramatically although secondary particle energy deposition as fraction of total energy deposition does not show such dramatic values, it should be noted, that in RBE calculations if secondary particles are included their individual contribution to total RBE should be weighed by energy deposition value rather than number of particles.

Further RBE calculations with secondary particle inclusion were not performed in this study, although from the data provided here it can be seen that the impact on RBE will be more pronounced for heavier particles as for protons the impact of secondary particles to total RBE values most likely are neglible. The secondary beam fragments should give rise to RBE near the end of the range near the Bragg peak and therefore at the SOBP distal edge. For such RBE calculation, a Monte Carlo simulation code should be created to score total energy deposition, primary particle energy deposition, secondary particle energy deposition grouped by atomic number of the particle and fluences of each particle group.

4 Conclusions

Drawing on results discussed in paragraphs of Chapter 3 the main conclusions of this study are:

1. When considering protons and heavy charged particles for medical cancer therapy purposes both physical and biological characteristics of particles need to be considered as dose deposition parameters physically and biologically can greatly differ.

2. Physical dose optimized spread-out Bragg peaks:

* heavier particle spread-out Bragg peaks exhibit higher entrance dose than protons;

* for varying peak length, therefore, tumour size entrance dose decreases with decreasing tumor size and the rate of this decrease is higher for lighter particles and deposited energy value at peak increases with decreasing tumor size;

* shallower spread-out Bragg peaks exhibit increased energy deposit compared to deep-seated peaks and entrance dose level changes for same peak length are different depending on particle type – higher for protons, dependent on tumor size for helium ions and lower for carbon and oxygen ions;

3. Biologically effective dose optimized spread-out Bragg peaks:

* uniform physical dose distributions result to non-uniform biological dose distributions in tissue, therefore biologically effective dose guided optimization should be used in design of spread-out Bragg peaks of heavy charged particles. Biological effects in this report were considered for the widely referenced human salivary gland cell line;

* heavy charged particles exhibit increased relative biological effectiveness (RBE) and RBE values tend to increase with increasing atomic number of particle – RBE values are similar for helium-3 and helium-4 ions and similarity can be also seen for carbon and oxygen ions;

* considering biological dose optimized spread-out Bragg peaks, helium ions exhibit entrance dose of about the same level or higher than protons, while carbon and oxygen ions exhibit decreased entrance dose level compared to protons, if prescribed dose level is 10 Gy or less;

* as RBE values are prescribed dose level dependent, entrance region relative dose levels depend on this dose level – with increasing dose entrance dose level also increases relative to peak;

* RBE values in entrance region are independent of spread-out Bragg peak length or depth, while RBE values at middle of peak and it's distal edge decrease with increasing SOBP length and are higher for deep-seated peaks than shallower;

* taking into consideration biological dose deposition effects in tissue, lower number of particles are necessary to achieve biologically effective dose of the same magnitude as physical dose and this effect mostly depends on RBE value, therefore exhibiting same dependencies;

* for increasing dose level, when considering biological dose a non-linear relationship between dose level and necessary number of particles is present, because of RBE value dependence on absorbed dose;

* for proper radiobiological effect calculations also secondary particle distributions should be considered as that could impact depth distribution of RBE values, what is more – because of this RBE values change in lateral beam dimensions as well compared to central axis.

4. Considering effectiveness of certain particle types:

* protons may exhibit effectiveness in terms of entrance dose level for high dose levels of about 20 Gy over other particles, but the effects of lateral spreading of the beam greatly limit this effectiveness;

* when considering helium ions – when biologically optimized spread-out Bragg peaks are considered, they exhibit the same or worse entrance dose characteristics as protons, but their lateral spread increases their effectiveness;

* when comparing helium-3 and helium-4 ions, helium-3 ions appear to be more beneficial for treatment – their radiobiological properties are equal, having the same RBE value for primary particles, but helium-3 ions exhibit better dose deposition characteristics as entrance region dose is lower than for helium-4 ions. Helium-4 ions exhibit smaller secondary fragment dose level close to distal edge of peak, but this difference is not significant (less than 1%);

* when considering carbon and oxygen ions – respective biologically optimized spread-out Bragg peaks exhibit lowest entrance dose levels among the studied particles for dose levels 2, 5 and 10 Gy, therefore indicating the best biological dose distributions among studied particles with the only drawback of fragmentation tail. It must be noted that carbon and oxygen ion effectiveness is more pronounced in deep-seated regions, in shallower depths the effectiveness over other particle types can be not significant and other particles could be more appropriate for treatment.

* when comparing carbon and oxygen ions – their RBE values calculated from primary particles are the same, dose deposition characteristics in entrance region appear to be the same and the only difference between these ion types is apparent in tail region – oxygen ions exhibit higher tail dose level close to distal edge of peak while at larger depths oxygen tail dose level becomes lower than carbon tail dose level. Studies also show that oxygen might exhibit better oxygen enhancment ratio, being applicable for hypoxic and radioresistant tumors.

5. FLASH effect modelling was not considered in itself of this study as there are no clear models as of yet, but studies show that FLASH effect in itself does not depend on particle type just on dose delivery time structure – dose per pulse, pulse repetition rate etc.

6. This study gives number of necessary particles for various cubic volumes both considering just the physical absorbed dose and biological effect corrected doses. These numbers can be used for constraints imposed on number of particles per spill in synchrotron design.

References

[1] Lin B, Gao F, Yang Y, et al. FLASH Radiotherapy: History and Future. *Front Oncol.* 2021;11:644400.

[2] Geant4 examples: Example Hadr01< https://geant4-userdoc.web.cern.ch/Doxygen/examples_doc/html/ExampleHadr01.html>

[3] Delmastro_ESIPAP2014_3.pptx

<https://indico.cern.ch/event/294651/contributions/671929/attachments/552041/760669/Delmastro_ESIPAP2014_3.pdf >

[4] Physical Reference Data | NIST <https://www.nist.gov/pml/productsservices/physical-reference-data>

[5] Comparison of Accelerator Designs for an Ion Therapy and Research Facility - CERN Document Server < https://cds.cern.ch/record/2748083>

[6] Physics1.pdf

< https://www.slac.stanford.edu/xorg/geant4/SLACTutorial14/Physics1.pdf>

[7] Guan F, Geng C, Ma D, Bronk L, Kerr M, Li Y, Gates D, Kroger B, Sahoo N, Titt U, Grosshans D, Mohan R. *RBE Model-Based Biological Dose Optimization for Proton Radiobiology Studies.* Int J Part Ther. 2018 Summer;5(1):160-171.

[8] INTERNATIONAL ATOMIC ENERGY AGENCY, Relative Biological Effectiveness in Ion Beam Therapy, Technical Reports Series No. 461, IAEA, Vienna, 2008

[9] Jones B. *A Simpler Energy Transfer Efficiency Model to Predict Relative Biological Effect for Protons and Heavier Ions* [published correction appears in Front Oncol. 2016;6:32]. Front Oncol. 2015

[10] The local effect model – principles and applications.

<https://three.jsc.nasa.gov/articles/LEM_20130426.pdf>

[11] Hawkins RB. *A microdosimetric-kinetic model of cell death from exposure to ionizing radiation of any LET, with experimental and clinical applications.* Int J Radiat Biol. 1996 Jun;69(6):739-55.

[12] Inaniwa T, Furukawa T, Kase Y, Matsufuji N, Toshito T, Matsumoto Y, Furusawa Y, Noda K. *Treatment planning for a scanned carbon beam with a*

modified microdosimetric kinetic model. Phys Med Biol. 2010 Nov 21;55(22):6721-37. doi: 10.1088/0031-9155/55/22/008. Epub 2010 Oct 28. PMID: 21030747.